



# WorldCup Sampling for Multi-bit LLM Watermarking

Yidan Wang<sup>1,2</sup> Yubing Ren<sup>1,2†</sup> Yanan Cao<sup>1,2</sup> Li Guo<sup>1,2</sup>

## Abstract

As large language models (LLMs) generate increasingly human-like text, watermarking offers a promising solution for reliable attribution beyond mere detection. While multi-bit watermarking enables richer provenance encoding, existing methods largely extend zero-bit schemes through seed-driven steering, leading to indirect information flow, limited effective capacity, and suboptimal decoding. In this paper, we propose WorldCup, a multi-bit watermarking framework for LLMs that treats sampling as a natural communication channel and embeds message bits directly into token selection via a hierarchical competition mechanism guided by complementary signals. Moreover, WorldCup further adopts entropy-aware modulation to preserve generation quality and supports robust message recovery through confidence-aware decoding. Comprehensive experiments show that WorldCup achieves a strong balance across capacity, detectability, robustness, text quality, and decoding efficiency, consistently outperforming prior baselines and laying a solid foundation for future LLM watermarking studies.

## 1. Introduction

Large language models (LLMs) (Guo et al., 2025; Comanici et al., 2025; Achiam et al., 2023) have shown remarkable performance across a wide range of real-world applications, including creative writing, code generation and AI agent (Luo et al., 2025), rendering LLM-generated text progressively indistinguishable from human-written text (Mitchell et al., 2023). While these advances significantly boost productivity, they also amplify serious risks such as misinformation dissemination, academic plagiarism, and phishing attacks (Tang et al., 2024). As a consequence, LLM watermarking has emerged as a promising approach to mitigate

<sup>1</sup>Institute of Information Engineering, Chinese Academy of Sciences, Beijing, China <sup>2</sup>School of Cyber Security, University of Chinese Academy of Sciences, Beijing, China. Correspondence to: Yubing Ren <renyubing@iie.ac.cn>.

Preprint. February 3, 2026.

these concerns by embedding imperceptible yet verifiable signals into generated text, thereby enabling reliable attribution, detection and traceability (Bengio et al., 2025).

Inference-time LLM watermarking can be broadly categorized into zero-bit and multi-bit based on embedding capacity (Liu et al., 2024b). While zero-bit watermarking focuses solely on detection, multi-bit watermarking further enables the extraction of rich metadata, such as model identity or generation timestamps. The prevailing multi-bit watermarking paradigm builds upon zero-bit schemes by implicitly embedding message into the stochastic generation process. Typically, a pseudo-random seed is derived by hashing a pre-defined secret key with the context and is associated with a target bit string to steer an underlying zero-bit watermarking mechanism, thereby establishing a verifiable link between the message and the generated text. Decoding reverses this process by searching over candidate messages to identify the one that best aligns the expected watermark signal.

However, this steering-based construction also exposes a deeper limitation of the current paradigm. Rather than writing the message directly into the generative process, existing methods route information through a multi-stage pathway: the message is first mapped to a seed, the seed induces a pseudo-random perturbation pattern, and only then does the perturbation manifest indirectly in the generated text. Such a long information chain inevitably incurs entropy loss at each stage, since the watermark signal must survive multiple transformations before reaching the surface form. In effect, the sampling process is treated as a binary detection probe rather than as a native communication channel, which restricts the usable capacity of each token. These constraints reflect the inherent difficulty of forcing a zero-bit mechanism to shoulder a multi-bit objective.

To overcome these limitations, we revisit multi-bit watermarking from a more direct and principled perspective. Rather than encoding messages indirectly through seed-driven steering, we treat the sampling step itself as a natural communication channel and embed bits directly into token selection. This shift is lightly motivated by Google’s SynthID Text (Dathathri et al., 2024), which demonstrates that token-ranking perturbations can leave statistically verifiable traces without degrading text quality, albeit in a detection-only setting. Building on this insight, we extend the idea to

a full-fledged multi-bit regime and introduce a multi-round, hierarchical sampling strategy that couples message embedding with the competitive selection of candidate tokens.

Specifically, we propose **WorldCup**, a multi-bit watermarking framework for LLMs that leverages the inherent redundancy of autoregressive token generation to support robust and scalable information embedding. At the **encoding** stage, WorldCup conceptualizes watermarking as a structured competition process, in which multiple complementary signals jointly guide token selection and induce stable statistical separation, while preserving sufficient flexibility for high-quality natural language generation. To balance detectability and fluency, the framework further incorporates an entropy-aware modulation mechanism that adaptively adjusts watermark strength in response to local uncertainty in the model output distribution. At the **decoding** stage, WorldCup moves beyond simple counting-based detection and adopts a confidence-aware aggregation strategy that weights token-level evidence by its statistical reliability, thereby mitigating the disproportionate influence of low-entropy tokens. These design choices enable fine-grained control over the divergence between clean and watermarked distributions, and become increasingly advantageous as the embedded payload grows, yielding substantial improvements in decoding accuracy and efficiency at scale.

To this end, comprehensive experiments across multiple LLMs and downstream tasks demonstrate that WorldCup consistently outperforms prior baselines, delivering a strong and well-balanced trade-off among multi-bit capacity, watermark detectability, robustness, text quality, and decoding efficiency. In summary, our contributions are threefold:

- We propose WorldCup, a versatile multi-bit watermarking framework that is rigorously validated through both theoretical analysis and extensive empirical evaluation.
- We introduce a confidence-aware decoding paradigm that moves beyond prior counting-based detectors, substantially improving both decoding accuracy and efficiency.
- We conduct a systematic analysis of key design components, examining different hyperparameter choices and offering actionable insights to guide future research.

## 2. Preliminaries

**Notations.** Consider an autoregressive LLM  $\Theta$  based on transformer (Vaswani et al., 2017), let  $\mathcal{V}$  denote the vocabulary set of all tokens with size  $|\mathcal{V}|$ . Given a prompt  $p_0$  and previously contextual tokens  $\mathbf{x}_{<t} = (x_1, x_2, \dots, x_{t-1})$ , the LLM generate an imminent token  $x_t \in \mathcal{V}$  sequentially from the conditional distribution  $P_\Theta(x_t | p_0, \mathbf{x}_{<t}) \in \Delta_{\mathcal{V}}$ . The process repeats until either a predefined maximum length is reached or an end-of-sequence token is produced.

### 2.1. SynthID-Text Zero-bit Watermarking

**Watermark Embedding.** For zero-bit watermarking SynthID-Text (Dathathri et al., 2024), at each generation step  $t$ , a random seed  $r_t$  is derived by hashing the previously generated text together with a secret watermark key  $\xi \in \Xi$ . The seed is then provided to  $m$  independent pseudo-random functions (PRFs)  $\mathbf{g} = (g_1, \dots, g_m)$  (Goldreich et al., 1986), each of which assigns a binary value  $g_\ell(x_i, r_t) \in \{0, 1\}$  to every token  $x_i \in \mathcal{V}$ , where  $\ell \in \{1, \dots, m\}$ . Token selection proceeds via an  $m$ -layer tournament-based sampling scheme. Concretely,  $N^m$  candidate tokens are independently sampled from the model distribution  $P_\Theta(\cdot | p_0, \mathbf{x}_{<t})$  to form the leaves of a complete  $N$ -ary tournament tree of depth  $m$ . At each layer  $\ell$ , candidates are grouped in sets of  $N$  and compared using the corresponding PRF scores  $g_\ell(\cdot, r_t)$ . In practice,  $N$  is set to 2, which corresponds to pairwise comparisons. The highest-scoring token in each group advances to the next layer, with ties broken at random. This elimination process continues until ultimately a single token remains, which is emitted as the output token  $x_t$ .

**Watermark Detection.** By design, tournament sampling biases the generation process toward tokens that attain higher scores under the watermarking functions  $\mathbf{g}$ . Given a generated text  $\mathbf{y} = (y_1, y_2, \dots, y_T)$ , watermark detection evaluates the degree to which the text  $\mathbf{y}$  aligns with the functions  $\mathbf{g}$ . Formally, the detection statistic is defined as the average watermark score over the sequence:

$$s(\mathbf{y}; \mathbf{g}) = \frac{1}{mT} \sum_{t=1}^T \sum_{\ell=1}^m g_\ell(y_t, r_t). \quad (1)$$

Since watermarked tokens are more likely to achieve higher  $g$ -values, watermarked texts are expected to exhibit significantly higher scores  $s(\mathbf{y}; \mathbf{g})$  than unwatermarked ones, enabling reliable statistical zero-bit watermarking detection.

### 2.2. MPAC Multi-bit Watermarking

Multi-bit Watermarking via Position Allocation (MPAC) (Yoo et al., 2024) extends zero-bit watermarking to the multi-bit setting by allocating generated tokens to message positions and encoding message bits through a classic zero-bit watermarking method KGW (Kirchenbauer et al., 2023).

**Message Encoding.** Let  $\mathbf{m} \in \sum^b$  denote the message to be embedded, where  $\sum = \{0, \dots, s-1\}$  is an  $s$ -ary alphabet (e.g.  $s = 2$  for binary messages) and  $b$  is the message length. At each generation step  $t$ , MPAC employs a PRF with random seed  $r_t$  to sample a message position  $p \in \{0, \dots, b-1\}$  and retrieves the corresponding message symbol  $\mathbf{m}[p]$ . Meanwhile, the vocabulary is randomly shuffled and partitioned into  $s$  disjoint subsets  $\mathcal{V}_t = [C_0, \dots, C_{s-1}]$ . According to the value of  $\mathbf{m}[p]$ , the

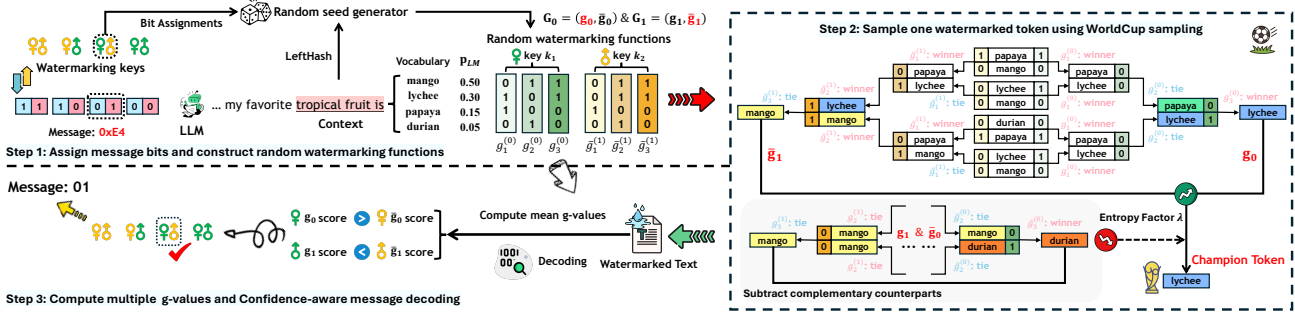


Figure 1. An overview of our multi-bit watermarking framework **WorldCup** for large language models.

corresponding subset is designated as the green list and is assigned a positive logits bias  $\delta$ . This bias increases the likelihood that LLM samples tokens from the designated subset, thereby embedding the message symbol during generation.

**Message Decoding.** MPAC extracts the embedded multi-bit messages from text via a majority voting matrix  $\mathbf{M} \in \mathbb{R}^{b \times s}$  initialized to zero. For each token  $y_t$ , the decoder reconstructs the message position  $p$  and the vocabulary partitions  $\mathcal{V}_t$  using the same PRF as in the encoding stage. If  $y_t \in C_j$ , the corresponding entry  $\mathbf{M}[p][j]$  is incremented by one. After processing the entire text, each message symbol is recovered via  $\hat{\mathbf{m}}[p] = \arg \max_{j \in \{0, \dots, s-1\}} (\mathbf{M}[p][j])$ . Under the assumption that watermarked text contains more green-list tokens than non-green-list tokens, the aggregate majority count  $\sum_{p=0}^{b-1} \max_j (\mathbf{M}[p][j])$  serves as the total green tokens for computing the  $z$ -score statistic, which subsequently determines whether the text is watermarked.

### 3. Methodology

**Overview.** As illustrated in Fig. 1, WorldCup framework comprises two central stages: message embedding and message decoding. We introduce the embedding methodology progressively. Section 3.1 presents a binary instantiation that embeds one bit per token using arbitrary  $g$ -value functions. Section 3.2 shows that complementary  $g$ -value functions achieve theoretically optimal performance, forming the core components of the framework. Building on this insight, Section 3.3 generalizes this formulation to embed  $k \geq 2$  bits per token. For decoding, Section 3.4 introduces a confidence-aware algorithm that aggregates fine-grained token-level evidence for robust and reliable message recovery.

#### 3.1. Binary WorldCup Watermarking

**Definition 3.1.** (random seed generator). Given a security parameter  $\kappa$ , define the random seed space as  $\mathcal{R} = \{0, 1\}^\kappa$ . Let  $h(\cdot)$  be a hash function and  $\xi$  a watermark key. At generation step  $t$ , the random seed is computed as

$$r_t = h(x_{t-c}, \dots, x_{t-1}, \xi) \in \mathcal{R}, \quad (2)$$

where  $c$  denotes the sliding-window size. We assume that  $r_t \sim \text{Unif}(\mathcal{R})$  for any  $x_{t-c}$  when  $\xi \sim \text{Unif}(\mathcal{R})$  with  $\text{Unif}(\cdot)$  represents the uniform distribution.

**Definition 3.2.** ( $g$ -value). Given a token  $x \in \mathcal{V}$ , a random seed  $r \in \mathcal{R}$ , and a layer index  $\ell \in \{1, \dots, m\}$ , a  $g$ -value function is a pseudo-random mapping  $g_\ell : \mathcal{V} \times \mathcal{R} \rightarrow \mathbb{R}$ . The  $g$ -value of token  $x$  at layer  $\ell$  is the random variable  $g_\ell(x, r)$ .

To implement binary WorldCup watermarking, we introduce two independent families of  $g$ -value functions  $\mathbf{g}_0 = (g_1^{(0)}, g_2^{(0)}, \dots, g_m^{(0)})$  and  $\mathbf{g}_1 = (g_1^{(1)}, g_2^{(1)}, \dots, g_m^{(1)})$ , to encode a binary message  $\mathbf{m} \in \{0, 1\}^b$ . At each generation step  $t$ , we first sample  $N^m$  (typically  $2^m$ ) candidate tokens  $\{y_0, y_1, \dots, y_{N-1}\}$  with replacement from the model distribution  $P_\Theta(\cdot | p_0, x_{t-c})$ . Then a cryptographic hash function  $h$  is applied to randomly assign the current token  $x_t$  to a target message bit, determining which bit is to be embedded.

Conditioned on the selected bit value, tournament sampling is carried out as follows. If the target bit equals 0, candidates are scored using the function family  $\mathbf{g}_0$ : at each tournament layer  $\ell$ , the score  $g_\ell^{(0)}(\cdot, r_t)$  is evaluated and the higher-scoring token advances to the next layer. This elimination process continues for  $m$  rounds, ultimately yielding a single winner  $x_t$ , which is emitted as the watermarked token. If the target bit equals 1, the same tournament structure is applied using the alternative family  $\mathbf{g}_1$ , as illustrated in Algorithm 1.

For efficiency, instead of explicitly running the tournament in Algorithm 1, we use an equivalent vectorized formulation to sample from the resulting watermarked distribution<sup>1</sup>:

**Definition 3.3.** (watermarked distribution). Given a probability distribution  $P_\Theta \in \Delta_{\mathcal{V}}$ , a random seed  $r_t \in \mathcal{R}$ , layers number  $m \geq 1$ , leaves number  $N \geq 2$  and  $g$ -value functions  $\mathbf{g}_0, \mathbf{g}_1$ . For message  $\mathbf{m}$ , position  $p$ , the watermarked distribution of the winner in Algorithm 1 is defined as:

$$q(x_t) = \mathbb{P}[\text{Alg. 1}(P_\Theta, r_t, m, N, \mathbf{m}[p], \mathbf{g}_0, \mathbf{g}_1) \Rightarrow x_t]. \quad (3)$$

Details and equivalence proofs are given in Appendix G.2.

<sup>1</sup>In general, we assume  $2^m \gg |\mathcal{V}|$ .

**Algorithm 1** Binary WorldCup Watermarking

```

1: Input: LLM distribution  $P_\Theta(\cdot | p_0, \mathbf{x}_{<t})$ , random seed
    $r_t$ , layers number  $m$ , leaves number  $N \geq 2$ , message
   bit  $\mathbf{m}[p]$ ,  $g$ -value function families  $\mathbf{g}_0, \mathbf{g}_1$ 
2: Draw  $N^m$  i.i.d tokens  $y_0^0, \dots, y_{N^m-1}^0 \sim P_\Theta(\cdot | p_0, \mathbf{x}_{<t})$ 
3: Initialize  $(g_1, \dots, g_m) \leftarrow \mathbf{g}_0$  if  $\mathbf{m}[p] = 0$  else  $\mathbf{g}_1$ 
4: for  $1 \leq \ell \leq m$  do
5:   for  $0 \leq j \leq N^{m-\ell} - 1$  do
6:      $Y := [y_j^{\ell-1}, \dots, y_{Nj+N+1}^{\ell-1}]$  // repeatable
7:      $Y^* := [y \in Y : g_\ell(y, r_t) = \max_{y' \in Y} g_\ell(y', r_t)]$ 
8:     Sample  $y_j^\ell \sim \text{Unif}(Y^*)$ 
9:   end for
10: end for
11: Return  $x_t \leftarrow y_0^m$ 

```

### 3.2. Complementary $g$ -value Functions

Thus far, the two  $g$ -value families have been treated as arbitrary pseudo-random constructions. We now consider a principled design in which  $\mathbf{g}_0$  and  $\mathbf{g}_1$  are constructed as complementary pairs, and show that this choice is optimal in terms of statistical discriminability.

**Definition 3.4.** (complementary  $g$ -value). Given a  $g$ -value  $g_\ell(x, r)$  as defined in Definition 3.2, its complementary  $g$ -value  $\bar{g}_\ell(x, r)$  is defined as follows:

$$\bar{g}_\ell(x, r) \triangleq 1 - g_\ell(x, r). \quad (4)$$

In this paper, we focus on the case where the  $g$ -value follows a Bernoulli distribution  $g_\ell(x, r) \sim \text{Bernoulli}(0.5)$ . Under this setting, both  $g_\ell(x, r)$  and  $\bar{g}_\ell(x, r)$  takes values in  $\{0, 1\}$ .

Intuitively, this complementary construction induces perfect anti-correlation between  $\mathbf{g}_0$  and  $\mathbf{g}_1$ : tokens favored under  $\mathbf{g}_0$  are deterministically disfavored under  $\mathbf{g}_1$ . As a result, the two message hypotheses are pushed to opposite extremes of the  $g$ -value spectrum, yielding the maximum possible separation between their induced embedding distributions. From a decoding perspective, this symmetry directly maximizes the decision margin and improves robustness against noise.

Figure 2 provides a visualization of this effect. Compared with independently sampled (random)  $g$ -value functions, complementary  $g$ -values exhibit a strict linear relationship, making the two message states (0 and 1) substantially easier to distinguish. This observation motivates the following proposition, which formalizes the optimality of complementary  $g$ -value functions in the multi-bit watermarking setting.

**Proposition 3.5.** Let  $g_\ell(x, r)$  be a Bernoulli  $g$ -value and  $\bar{g}_\ell(x, r)$  its complementary counterpart. Encoding bits 0 and 1 by selecting between  $g_\ell$  and  $\bar{g}_\ell$  yields two embedding distributions whose statistical discriminability is maximized.

A formal proof based on the maximization of the expected

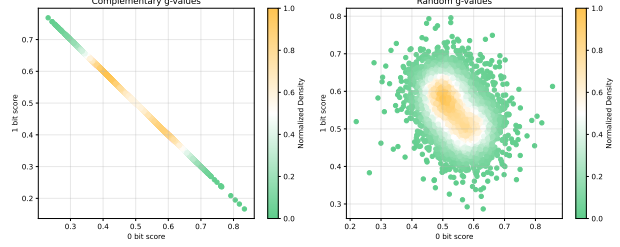


Figure 2. Binary complementary  $g$ -values vs. random  $g$ -values.

squared difference  $\mathbb{E}[(\mathbf{g}_1 - \mathbf{g}_0)^2]$  and an explicit correlation analysis are deferred to Appendix G.1.

### 3.3. Generalized WorldCup Watermarking

While binary WorldCup sampling enables the embedding of one bit per token, the allocation of information across tokens can become increasingly imbalanced as the message length grows (Qu et al., 2025). Although the nominal per-token capacity remains fixed, the global utilization of token-level degrees of freedom is therefore suboptimal. To more fully exploit the information-carrying potential of each token, we generalize the WorldCup framework by introducing  $k$  groups of  $g$ -value function families, allowing each token to simultaneously encode  $k$  bits.

We consider the simplest but nontrivial setting where each token carries two bits (i.e.  $k = 2$ ). To this end, we sample two independent families of  $g$ -value functions, denoted by  $\mathbf{G}_0 = (\mathbf{g}_0, \bar{\mathbf{g}}_0)$  and  $\mathbf{G}_1 = (\mathbf{g}_1, \bar{\mathbf{g}}_1)$ . The first bit is encoded using  $\mathbf{G}_0$ , following the binary setting: when the bit equals 0, the watermark distribution  $q_0$  (defined in Definition 3.3) is derived from  $\mathbf{g}_0$ ; otherwise, its complementary function  $\bar{\mathbf{g}}_0$  is applied, yielding the distribution  $\bar{q}_0$ . The second bit is encoded analogously using  $\mathbf{G}_1$ , producing either  $q_1$  or  $\bar{q}_1$ .

Conceptually, a token that correctly embeds both bits should score highly under both corresponding  $g$ -value functions. We thus aggregate their distributions additively. However,  $\mathbf{G}_0$  and  $\mathbf{G}_1$  are independent rather than mutually exclusive, so naive aggregation yields limited separability between bit patterns. To enhance discriminability, we subtract contributions from complementary distributions, thereby sharpening the contrast between competing message hypotheses. In terms of tournament sampling, this strategy favors tokens that rank highly under the intended  $g$ -value functions while ranking poorly under their complementary counterparts.

Although this more aggressive separation improves detectability, it can also distort the underlying language model distribution and degrade text quality, as demonstrated in Section 5.1. To strike a better balance between detectability and fluency, we introduce an entropy-aware dynamic adjustment factor. Concretely, for a two-bit message  $\mathbf{m}'$ , we define the

updated watermarked scores as follows:

$$P_{\Theta, \mathbf{m}} = \begin{cases} (q_0 + q_1) - \lambda(\bar{q}_0 + \bar{q}_1), & \mathbf{m}' = 00 \\ (q_0 + \bar{q}_1) - \lambda(\bar{q}_0 + q_1), & \mathbf{m}' = 01 \\ (\bar{q}_0 + q_1) - \lambda(q_0 + \bar{q}_1), & \mathbf{m}' = 10 \\ (\bar{q}_0 + \bar{q}_1) - \lambda(q_0 + q_1), & \mathbf{m}' = 11 \end{cases}. \quad (5)$$

The scores are log-transformed for numerical stability and normalized via softmax, from which the **champion token** is ultimately sampled. Here, the coefficient  $\lambda$  is adaptively determined by the entropy of the base LLM distribution:

$$\lambda = \alpha \cdot \sigma(\sum -P_{\Theta} \log P_{\Theta}), \quad (6)$$

where  $\alpha$  is a hyperparameter that controls the watermark strength, and  $\sigma$  denotes the activation function, with their specific choices reported in Appendix I.5. Under this formulation, high-entropy (low-confidence) token positions permit stronger separation, while low-entropy tokens favor more conservative modulation to preserve generation quality.

This construction can be naturally generalized to  $k > 2$  groups of  $g$ -value functions, allowing each token to embed  $k$  bits. Detailed formulations are provided in Appendix G.3.

### 3.4. Confidence-aware Message Decoding

In contrast to prior counting-based decoding, our method employs a confidence-aware strategy that aggregates fine-grained token-level scores across groups associated with the same message position, rather than making hard binary decisions per token. This design yields substantially more stable detection statistics, as illustrated in Fig. 3.

**Problem setup.** Let  $\mathbf{y}_{1:T} = (y_1, y_2, \dots, y_T)$  denote a generated text sequence of length  $T$ . As in the encoding stage, we consider  $k$  independent groups of  $g$ -value function families  $\{\mathbf{G}_j = (\mathbf{g}_j, \bar{\mathbf{g}}_j)\}_{j=1}^k$ . These  $k$  families jointly encode a  $k$ -bit message string at each token position. Accordingly, a binary message  $\{0, 1\}^b$  is reparameterized as a sequence of  $2^k$ -ary message  $\mathbf{m} = (m_0, \dots, m_{B-1})$ ,  $m_p \in \{0, \dots, 2^k - 1\}$  where  $p \in \{0, \dots, B-1\}$  and  $B = b/k$  denotes the total number of message symbols.

**1) Recovering message positions.** We first employ the same hash function and watermarking key used during message embedding stage to identify the message bit position  $p$  associated with each token  $y_t$ . All tokens assigned to the same index  $p$  are then grouped together for joint decoding of the corresponding  $2^k$ -ary symbol  $m_p$ .

**2) Computing confidence scores.** For each message position  $p$  and each group  $j \in \{1, \dots, k\}$ , we compute the empirical mean  $g$ -values over the associated token group, following Eq. 1. Specifically, we obtain  $s_j^p$  and  $\bar{s}_j^p$  corresponding to  $\mathbf{g}_j$  and  $\bar{\mathbf{g}}_j$ , respectively. These quantities serve

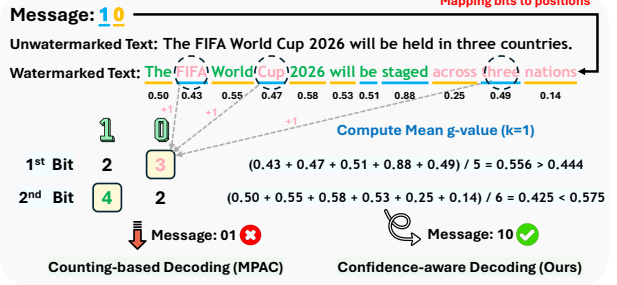


Figure 3. The comparison of multi-bit message decoding.

as confidence scores indicating whether the  $j$ -th bit of the  $2^k$ -ary message symbol at position  $p$  favors 0 or 1.

**3) Extracting message symbols.** For each message position  $p$ , we independently infer the  $j$ -th bit of the embedded symbol by comparing  $s_j^p$  and  $\bar{s}_j^p$ . The recovered  $2^k$ -ray message symbol  $\hat{m}_p \in \{0, \dots, 2^k - 1\}$  is then obtained as

$$\hat{m}_p = \sum_{j=1}^k 2^{k-j} \mathbb{I}(s_j^p < \bar{s}_j^p). \quad (7)$$

**Computing the watermark  $z$ -score.** We formulate watermark detection as a hypothesis test under the null hypothesis that the text is unwatermarked. Detection is based on a standardized  $z$ -score, whose definition and derivation are provided in Appendix G.4. Under the null hypothesis, unwatermarked texts yield low  $z$ -score, whereas watermarked texts produce systematically larger values. Consequently, a sufficiently large  $z$ -score leads to rejection of the null hypothesis, indicating the presence of a watermark.

## 4. Experiments

**Overview.** We conduct a comprehensive empirical evaluation of WorldCup along three fundamental dimensions: **message embedding capacity** (Section 4.2), **text quality** (Section 4.4), and **robustness** (Section 4.4).

### 4.1. Experimental Setup

**Baselines.** We compare WorldCup with representative multi-bit LLM watermarking methods that are publicly available, model-agnostic, and training-free, including BiMark (Feng et al., 2025), MPAC (Yoo et al., 2024), and SegMark (Qu et al., 2025). Message lengths are set to 16, 24, 32, and 48 bits. Detailed settings are in Appendix B.

**Datasets.** Following prior work (Kirchenbauer et al., 2023; Zhao et al., 2024), we randomly sample 200 prompts from the C4 (Raffel et al., 2020) and OpenGen (Krishna et al., 2023) datasets for text generation. We further evaluate

Table 1. Comparison of different multi-bit watermark performance, where  $\mathcal{O}$  denotes the baselines,  $\mathcal{C}$  denotes our watermark method.

Bit Length	Watermark	LLAMA3-8B-BASE								GEMMA2-9B-BASE							
		MAX 128 TOKENS				MAX 256 TOKENS				MAX 128 TOKENS				MAX 256 TOKENS			
		AUC $\uparrow$	Bit Acc $\uparrow$	PPL $\downarrow$	Time (s) $\downarrow$	AUC $\uparrow$	Bit Acc $\uparrow$	PPL $\downarrow$	Time (s) $\downarrow$	AUC $\uparrow$	Bit Acc $\uparrow$	PPL $\downarrow$	Time (s) $\downarrow$	AUC $\uparrow$	Bit Acc $\uparrow$	PPL $\downarrow$	Time (s) $\downarrow$
16 bits	$\mathcal{O}$ MPAC	0.999	0.960	16.25	0.049	0.996	0.980	13.56	0.087	0.980	0.920	13.69	0.045	0.985	0.940	12.00	0.070
	$\mathcal{O}$ SegMark	0.993	0.948	15.88	0.551	0.995	0.999	12.94	0.839	0.979	0.895	13.19	1.234	0.999	0.977	10.94	2.402
	$\mathcal{O}$ BiMark	1.000	0.977	14.34	0.026	1.000	0.987	11.25	0.044	1.000	0.929	11.06	0.031	0.999	0.955	9.625	0.039
	$\mathcal{C}$ Ours ( $k = 1$ )	1.000	0.975	8.000	0.008	1.000	0.986	6.703	0.012	0.993	0.909	6.750	0.008	1.000	0.951	5.719	0.011
	$\mathcal{C}$ Ours ( $k = 2$ )	0.999	0.982	12.94	0.009	1.000	0.990	11.25	0.015	0.998	0.931	10.84	0.008	0.998	0.956	8.906	0.012
24 bits	$\mathcal{O}$ MPAC	0.996	0.916	16.75	0.052	0.997	0.955	14.00	0.074	0.972	0.875	13.69	0.044	0.959	0.905	12.00	0.070
	$\mathcal{O}$ SegMark	0.947	0.839	17.13	0.721	0.992	0.992	13.38	0.804	0.849	0.734	13.19	1.670	0.974	0.922	10.13	2.853
	$\mathcal{O}$ BiMark	1.000	0.941	14.34	0.027	1.000	0.970	11.34	0.036	0.998	0.875	11.63	0.030	0.990	0.921	9.938	0.043
	$\mathcal{C}$ Ours ( $k = 1$ )	1.000	0.931	8.125	0.008	1.000	0.963	6.625	0.014	0.998	0.880	7.078	0.008	0.998	0.916	5.844	0.013
	$\mathcal{C}$ Ours ( $k = 2$ )	1.000	0.943	13.69	0.009	1.000	0.972	11.53	0.014	0.998	0.894	10.44	0.008	0.999	0.925	8.625	0.012
32 bits	$\mathcal{O}$ MPAC	0.997	0.890	16.75	0.051	0.996	0.939	14.00	0.090	0.947	0.837	13.81	0.046	0.940	0.869	11.63	0.074
	$\mathcal{O}$ SegMark	0.909	0.802	16.63	0.642	0.989	0.964	12.94	1.053	0.824	0.691	12.75	1.751	0.955	0.868	10.25	3.362
	$\mathcal{O}$ BiMark	1.000	0.890	13.91	0.026	1.000	0.947	12.38	0.040	0.996	0.806	12.00	0.031	0.989	0.865	9.938	0.041
	$\mathcal{C}$ Ours ( $k = 1$ )	0.999	0.893	7.813	0.009	1.000	0.940	6.688	0.013	0.990	0.842	7.094	0.008	0.995	0.885	5.906	0.013
	$\mathcal{C}$ Ours ( $k = 2$ )	1.000	0.915	13.38	0.010	1.000	0.958	11.25	0.017	0.995	0.859	10.94	0.009	0.994	0.905	8.688	0.013
48 bits	$\mathcal{O}$ MPAC	0.993	0.828	16.63	0.057	0.990	0.891	13.19	0.078	0.936	0.770	14.00	0.048	0.914	0.821	12.19	0.076
	$\mathcal{O}$ SegMark	0.837	0.628	16.38	0.725	0.968	0.848	13.56	1.381	0.770	0.600	13.38	2.668	0.900	0.697	9.938	3.382
	$\mathcal{O}$ BiMark	1.000	0.783	14.25	0.027	0.999	0.880	11.63	0.037	0.985	0.688	11.53	0.029	0.975	0.767	10.03	0.040
	$\mathcal{C}$ Ours ( $k = 1$ )	0.997	0.838	7.938	0.011	1.000	0.897	6.594	0.014	0.987	0.768	6.875	0.009	0.994	0.822	5.656	0.014
	$\mathcal{C}$ Ours ( $k = 2$ )	1.000	0.862	13.69	0.011	1.000	0.916	11.63	0.017	0.993	0.800	10.34	0.010	0.989	0.851	9.063	0.015

downstream performance on four representative tasks: machine translation, text summarization, question answering, and math reasoning. More details are in Appendix C.

**Metrics.** We primarily use Bit Accuracy to evaluate message decoding correctness. Detectability is measured using AUC and Best F1 score, while text quality is assessed with Median Perplexity (PPL), ROUGE-L, BLEU, Pass@1, and the GPT-4 Score. Robustness is evaluated using AUROC curves. Metric definitions are provided in Appendix D.

**Models.** For detectability and robustness evaluation, we use LLaMA3-8B-Base (Grattafiori et al., 2024) and Gemma2-9B-Base (Team et al., 2024). For downstream tasks, we additionally evaluate their Instruct-tuned variants and the latest Minstral-8B-Instruct (Liu et al., 2026). For fairness, we compute PPL using the larger Vicuna-13B-v1.5 model (Chiang et al., 2023). The details are in Appendix E.

**Implementation Details.** Our method is implemented in Python 3.10.0 with PyTorch 2.6.0. All experiments are conducted on a single NVIDIA A100 80 GB GPU. We use a default setup with temperature = 1.0, top-k = 50, top-p = 0.95, no\_repeat\_ngram\_size = 4, layers number  $m = 30$ , and  $\alpha = 1.2$ , together with *leffhash* and window size  $c = 2$ .

## 4.2. Message Embedding Capacity

Overall, we evaluate watermark detectability with different numbers of  $g$ -value functions, using  $k = 1$  and  $k = 2$  to embed 1-bit and 2-bit per token, respectively. Across all settings, WorldCup delivers both reliable watermark detection and accurate bit recovery, even as payload scales up.

**Multi-bit watermarking scenario.** We evaluate message decoding performance under maximum sequence lengths

of 128 and 256 tokens, with the minimum length fixed at 64. Table 1 shows that WorldCup consistently outperforms all baselines across both backbones. For LLaMA3-8B with 128-token sequences, WorldCup ( $k = 1$ ) improves bit accuracy by **2.7%**, **9.2%**, **9.1%**, and **21%** for 16-bit, 24-bit, 32-bit, and 48-bit messages, respectively, compared to SegMark. For Gemma2-9B, WorldCup ( $k = 2$ ) achieves average gains of **2.3%** and **3.9%** over MPAC and BiMark across all settings. Overall, these results indicate the effectiveness of WorldCup, where incorporating multiple  $g$ -functions improves per-token information utilization and leads to more reliable message recovery. We further observe that BiMark, MPAC, SegMark, WorldCup ( $k = 1$ ), and WorldCup ( $k = 2$ ) exhibit lower average decoding accuracy on Gemma2-9B than LLaMA3-8B, with decreases of **7.1%**, **5.3%**, **8.0%**, **5.6%**, and **5.2%**, respectively. This gap is likely due to stronger generation capability, which reduces token-level uncertainty and details are in Appendix I.1.

**Zero-bit watermarking scenario.** Using the method described in Section 3.4 to compute the  $z$ -score as the detection statistic, WorldCup achieves an average AUC of approximately **99.7%** across all scenarios. Moreover, 256-token sequences consistently outperform 128-token sequences, highlighting that longer contexts naturally accumulate stronger statistical evidence. These results not only confirm that detectability remains stable under large payloads, but also demonstrate that WorldCup gracefully subsumes the zero-bit watermarking regime without additional mechanisms.

## 4.3. Text Quality Preservation

**Perplexity (PPL).** As shown in Table 1 and Fig. 7, WorldCup consistently achieves lower perplexity than existing baselines, indicating strong text fluency preservation. We also observe that generated sequences with increased length

Table 2. The performance of various watermarking algorithms across four different downstream tasks on three instruct-tuned LLMs.

Model	Task 1: Short Q, Short A Machine Translation			Task 2: Long Q, Short A Text Summarization			Task 3: Short Q, Long A Long-form QA			Task 4: Long Q, Long A Math Reasoning		
	Best F1 $\uparrow$	Bit Accuracy $\uparrow$	BLEU $\uparrow$	Best F1 $\uparrow$	Bit Accuracy $\uparrow$	ROUGE-1 $\uparrow$	Best F1 $\uparrow$	Bit Accuracy $\uparrow$	GPT4 Score $\uparrow$	Best F1 $\uparrow$	Bit Accuracy $\uparrow$	Pass@1 $\uparrow$
+ Watermark	-	-	0.200 $\pm$ 0.002	-	-	0.221 $\pm$ 0.001	-	-	5.250 $\pm$ 0.073	-	-	0.340 $\pm$ 0.010
<b>MINISTRAL-8B-IT</b>	-	-	0.240 $\pm$ 0.002	-	-	0.215 $\pm$ 0.001	0.946 $\pm$ 0.002	0.879 $\pm$ 0.001	5.122 $\pm$ 0.029	0.785 $\pm$ 0.002	0.879 $\pm$ 0.001	0.265 $\pm$ 0.000
+ MPAC	0.745 $\pm$ 0.005	0.886 $\pm$ 0.004	0.166 $\pm$ 0.001	0.951 $\pm$ 0.003	0.929 $\pm$ 0.002	0.215 $\pm$ 0.001	0.946 $\pm$ 0.002	0.879 $\pm$ 0.001	5.122 $\pm$ 0.029	0.785 $\pm$ 0.002	0.879 $\pm$ 0.001	0.265 $\pm$ 0.000
+ BiMark	0.776 $\pm$ 0.006	0.803 $\pm$ 0.030	0.193 $\pm$ 0.003	0.977 $\pm$ 0.005	0.943 $\pm$ 0.005	0.208 $\pm$ 0.002	0.992 $\pm$ 0.000	0.894 $\pm$ 0.002	4.998 $\pm$ 0.088	0.767 $\pm$ 0.006	0.877 $\pm$ 0.002	0.310 $\pm$ 0.050
+ WorldCup ( $k = 1$ )	0.672 $\pm$ 0.000	0.793 $\pm$ 0.000	0.221 $\pm$ 0.000	0.967 $\pm$ 0.008	0.948 $\pm$ 0.002	0.231 $\pm$ 0.002	0.977 $\pm$ 0.003	0.871 $\pm$ 0.003	5.319 $\pm$ 0.008	0.777 $\pm$ 0.002	0.854 $\pm$ 0.002	0.355 $\pm$ 0.000
+ WorldCup ( $k = 2$ )	0.752 $\pm$ 0.004	0.919 $\pm$ 0.009	0.202 $\pm$ 0.005	0.983 $\pm$ 0.001	0.955 $\pm$ 0.002	0.213 $\pm$ 0.004	0.996 $\pm$ 0.001	0.905 $\pm$ 0.002	5.207 $\pm$ 0.092	0.898 $\pm$ 0.000	0.953 $\pm$ 0.000	0.315 $\pm$ 0.000
<b>LLaMA3.1-8B-IT</b>	-	-	0.268 $\pm$ 0.004	-	-	0.249 $\pm$ 0.001	-	-	5.243 $\pm$ 0.069	-	-	0.500 $\pm$ 0.020
+ MPAC	0.700 $\pm$ 0.000	0.805 $\pm$ 0.002	0.224 $\pm$ 0.002	0.880 $\pm$ 0.010	0.869 $\pm$ 0.004	0.249 $\pm$ 0.002	0.940 $\pm$ 0.003	0.855 $\pm$ 0.003	5.110 $\pm$ 0.052	0.856 $\pm$ 0.006	0.927 $\pm$ 0.004	0.343 $\pm$ 0.007
+ BiMark	0.718 $\pm$ 0.002	0.768 $\pm$ 0.061	0.258 $\pm$ 0.005	0.960 $\pm$ 0.004	0.898 $\pm$ 0.004	0.242 $\pm$ 0.001	0.981 $\pm$ 0.000	0.872 $\pm$ 0.003	5.066 $\pm$ 0.110	0.868 $\pm$ 0.005	0.922 $\pm$ 0.006	0.420 $\pm$ 0.020
+ WorldCup ( $k = 1$ )	0.672 $\pm$ 0.000	0.768 $\pm$ 0.000	0.315 $\pm$ 0.000	0.912 $\pm$ 0.006	0.860 $\pm$ 0.004	0.261 $\pm$ 0.003	0.957 $\pm$ 0.006	0.843 $\pm$ 0.004	5.258 $\pm$ 0.062	0.814 $\pm$ 0.009	0.917 $\pm$ 0.004	0.468 $\pm$ 0.012
+ WorldCup ( $k = 2$ )	0.705 $\pm$ 0.003	0.850 $\pm$ 0.025	0.272 $\pm$ 0.001	0.963 $\pm$ 0.004	0.919 $\pm$ 0.006	0.247 $\pm$ 0.002	0.986 $\pm$ 0.000	0.882 $\pm$ 0.005	5.149 $\pm$ 0.024	0.892 $\pm$ 0.003	0.947 $\pm$ 0.001	0.445 $\pm$ 0.005
<b>GEMMA2-9B-IT</b>	-	-	0.407 $\pm$ 0.001	-	-	0.312 $\pm$ 0.002	-	-	6.027 $\pm$ 0.093	-	-	0.650 $\pm$ 0.010
+ MPAC	0.673 $\pm$ 0.000	0.686 $\pm$ 0.007	0.393 $\pm$ 0.002	0.671 $\pm$ 0.000	0.619 $\pm$ 0.001	0.309 $\pm$ 0.001	0.838 $\pm$ 0.000	0.770 $\pm$ 0.001	5.920 $\pm$ 0.003	0.670 $\pm$ 0.000	0.670 $\pm$ 0.000	0.625 $\pm$ 0.000
+ BiMark	0.675 $\pm$ 0.002	0.606 $\pm$ 0.027	0.398 $\pm$ 0.002	0.669 $\pm$ 0.000	0.598 $\pm$ 0.011	0.317 $\pm$ 0.003	0.883 $\pm$ 0.004	0.762 $\pm$ 0.001	5.946 $\pm$ 0.027	0.676 $\pm$ 0.002	0.706 $\pm$ 0.003	0.590 $\pm$ 0.000
+ WorldCup ( $k = 1$ )	0.668 $\pm$ 0.000	0.623 $\pm$ 0.000	0.417 $\pm$ 0.001	0.671 $\pm$ 0.000	0.627 $\pm$ 0.001	0.318 $\pm$ 0.001	0.831 $\pm$ 0.004	0.760 $\pm$ 0.001	6.182 $\pm$ 0.003	0.676 $\pm$ 0.002	0.659 $\pm$ 0.005	0.630 $\pm$ 0.010
+ WorldCup ( $k = 2$ )	0.673 $\pm$ 0.002	0.713 $\pm$ 0.002	0.361 $\pm$ 0.003	0.668 $\pm$ 0.001	0.664 $\pm$ 0.001	0.312 $\pm$ 0.001	0.886 $\pm$ 0.001	0.800 $\pm$ 0.002	6.136 $\pm$ 0.017	0.678 $\pm$ 0.005	0.755 $\pm$ 0.010	0.600 $\pm$ 0.020

tend to yield lower PPL. For instance, compared to 128-token sequences, longer 256-token sequences generated by WorldCup ( $k = 2$ ) achieve average PPL reductions of **2.01** and **1.82** in LLaMA3-8B and Gemma2-9B, respectively. Notably, WorldCup ( $k = 1$ ) even attains a PPL lower than that of natural text, suggesting that it implicitly regularizes generation and effectively mitigates distributional shifts from original LLM. Additional hyperparameter effects on PPL, such as *no\_repeat\_ngram\_size*, are reported in Appendix I.6.

**Downstream Task Performance.** As summarized in Table 2, WorldCup ( $k = 1$ ) achieves the strongest overall performance across nearly all tasks. In particular, it improves Machine Translation and Text Summarization by an average of **2.6%** and **0.93%**, respectively, compared with non-watermarked baselines. This advantage stems from its multi-round tournament sampling mechanism, which robustly preserves the quality of generated text. Meanwhile, WorldCup ( $k = 2$ ) attains the highest multi-bit decoding accuracy and outperforms previous baselines on several tasks, especially those involving longer outputs. For example, in the long-form QA task, it surpasses MPAC by an average of **2.6%**, **2.7%**, and **3.0%** on Ministral, LLaMA3.1, and Gemma2, respectively. At the same time, on the LLaMA3.1-8B-IT model, WorldCup ( $k = 2$ ) outperforms BiMark by **1.4%**, **0.5%**, **8.3%**, and **2.5%** across four downstream task metrics. These results demonstrate that our method not only achieves high decoding reliability but also maintains superior text quality, allowing flexible trade-offs to select the optimal strategy for specific downstream tasks.

#### 4.4. Robustness to Real-world Attacks

**Attack Settings.** We assess robustness under three common attacks (Kirchenbauer et al., 2024): editing (word deletion and synonym substitution), copy-paste, and paraphrasing using Dipper (Krishna et al., 2023) using 256-token watermarked texts. Full settings are provided in Appendix F.

As shown in Fig. 4, Fig. 8, and Fig. 9, WorldCup consis-

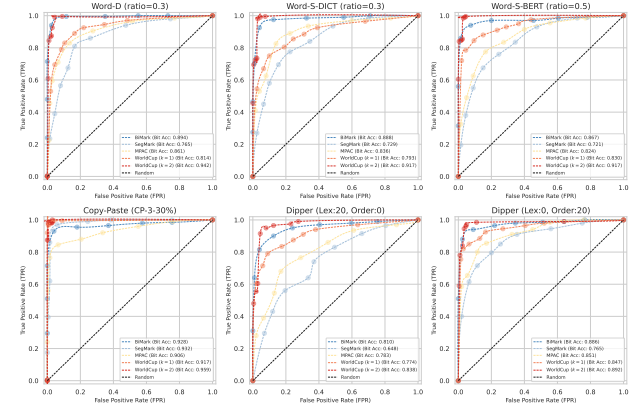


Figure 4. The AUROC curves under different attacks on LLaMA3.

tently outperforms existing watermarking methods across a variety of attack scenarios, achieving higher AUC scores and decoding accuracy. In the six attack scenarios illustrated in Fig. 4, WorldCup ( $k = 2$ ) attains an average AUC of **98.9%** and a decoding accuracy of **91.1%**, surpassing BiMark, MPAC, and SegMark by **3.2%**, **6.7%**, and **15.1%**, respectively. This robustness arises from its ability to more effectively leverage per-token redundancy to encode multiple bits, ensuring that a sufficient watermark signal remains even under substantial perturbations. Intuitively, as the number of embedded message bits increases, longer text sequences are required to achieve reliable message extraction and watermark detection; otherwise, fewer tokens per bit may lead to reduced robustness. We further investigate the effect of the hash window size in Appendix I.6, demonstrating that increasing the window size diminishes robustness due to reduced locality in watermark signal aggregation.

## 5. Further Analysis

### 5.1. Ablation Study

**Settings.** To understand the contribution of each design choice in WorldCup ( $k = 2$ ), i.e.,  $q - \lambda \bar{q}$ , where  $q$  denotes

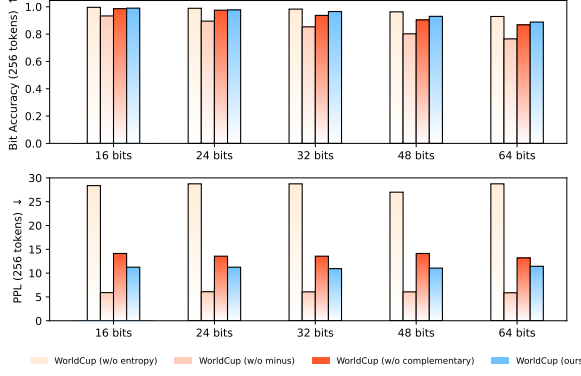


Figure 5. The ablation study of WorldCup ( $k = 2$ ) on LLaMA3.

the distribution induced by  $k$  groups of  $g$ -value functions, we perform a component-wise ablation study. We evaluate three variants: (i) removing the entropy-aware dynamic adjustment factor  $\lambda$  (**WorldCup w/o entropy**, i.e.,  $q - \bar{q}$ ); (ii) disabling the subtraction of complementary  $g$ -value distributions (**WorldCup w/o minus**, i.e.,  $q$ ); and (iii) replacing complementary  $g$ -value functions with randomly sampled ones (**WorldCup w/o complementary**, i.e.,  $q - \lambda q'$ ).

As shown in Fig. 5, the entropy-aware factor plays a crucial role in preserving text quality. Although it slightly reduces bit decoding accuracy, it substantially lowers the PPL of the generated text. In contrast, directly sampling from the original  $g$ -values without subtracting their complementary counterparts achieves relatively low PPL, but suffers from poor discriminability, which significantly degrades decoding accuracy. Finally, when embedding either bit 0 or bit 1, using complementary  $g$ -value functions consistently outperforms random  $g$ -value functions in terms of both decoding accuracy and text quality. This observation is fully aligned with our theoretical analysis in Appendix G.4. Overall, these results validate the necessity of each component and highlight their synergistic effect.

## 5.2. Computational Cost Analysis

For **encoding**, we evaluate the encoding time and bit accuracy when embedding  $k$  bits *per token* using  $k$  groups of  $g$ -value functions, as shown in Fig. 6. We observe that increasing  $k$  leads to a roughly linear increase in encoding time. Specifically, generating a single token takes **0.08s** when  $k = 1$ , while the time increases to **0.69s** when  $k = 8$ . Meanwhile, increasing  $k$  does not monotonically improve decoding accuracy, as the information capacity of each token is inherently limited. In practice, the best performance is typically achieved at  $k = 2$ . For **decoding**, we quantify the *per sample* decoding time, defined as the time required to decode one complete generated text, including both  $z$ -score computation and multi-bit message recovery. The results

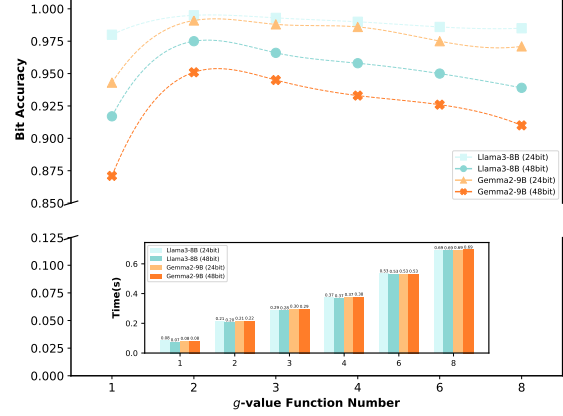


Figure 6. The effect of embedding  $k$  bits in each token.

are reported in Table 1. WorldCup achieves the highest decoding efficiency, requiring approximately **1 ~ 2 ms** on average to decode a single watermarked text. This efficiency advantage arises from confidence-aware decoding, which enables fully parallel aggregation of  $g$ -values and removes the need for token counting. As a result, WorldCup scales favorably to longer sequences and higher payloads, highlighting its suitability for practical large-scale deployment.

## 5.3. Different Watermark Functions and Detectors

We further examine how different  $g$ -value functions and detectors affect multi-bit watermark performance. Non-distortionary  $g$ -value functions preserve the sampling distribution in expectation and thus improve text quality, but they substantially reduce watermark detectability and multi-bit decoding accuracy, as shown in Appendix I.2. We also observe that weighted-mean detectors perform better when  $k = 1$ , whereas mean detectors are more effective for  $k = 2$ , as detailed in Appendix I.3. This may be because combining multiple  $g$ -value functions smooths layer-wise effects and mitigates sensitivity to tournament depth, with supporting experiments on varying sampling layers  $m$  in Appendix I.4.

## 6. Conclusion

We introduced WorldCup, a novel multi-bit watermarking framework for LLMs that treats inference-time sampling as a communication channel for structured information embedding. By integrating complementary watermarking signals with entropy-aware modulation and confidence-aware decoding, WorldCup enables robust and scalable message embedding without compromising text quality. Experiments across diverse models and tasks demonstrate clear advantages over existing baselines in accuracy, efficiency, and robustness. We believe that WorldCup provides a principled foundation for scalable multi-bit watermarking and supports practical deployment for reliable LLM content attribution.

## Impact Statement

This paper presents WorldCup, a multi-bit watermarking framework for large language models that enables reliable content attribution and integrity verification. By supporting robust message embedding while preserving text quality, WorldCup promotes accountable and transparent LLM deployment. At the same time, we acknowledge potential risks such as privacy concerns or misuse for surveillance and encourage responsible research and governance to ensure watermarking serves transparency and user rights.

## References

Aaronson, S. Watermarking of large language models. In *Large Language Models and Transformers Workshop at Simons Institute for the Theory of Computing*, 2023., 2023. URL <https://www.youtube.com/watch?v=2Kx9jbSMZqA>.

Achiam, J., Adler, S., Agarwal, S., Ahmad, L., Akkaya, I., Aleman, F. L., Almeida, D., Altenschmidt, J., Altman, S., Anadkat, S., et al. Gpt-4 technical report. *arXiv preprint arXiv:2303.08774*, 2023.

Barrault, L., Bojar, O., Costa-jussà, M. R., Federmann, C., Fishel, M., Graham, Y., Haddow, B., Huck, M., Koehn, P., Malmasi, S., Monz, C., Müller, M., Pal, S., Post, M., and Zampieri, M. Findings of the 2019 conference on machine translation (WMT19). In Bojar, O., Chatterjee, R., Federmann, C., Fishel, M., Graham, Y., Haddow, B., Huck, M., Yepes, A. J., Koehn, P., Martins, A., Monz, C., Negri, M., Névéol, A., Neves, M., Post, M., Turchi, M., and Verspoor, K. (eds.), *Proceedings of the Fourth Conference on Machine Translation (Volume 2: Shared Task Papers, Day 1)*, pp. 1–61, Florence, Italy, August 2019. Association for Computational Linguistics. doi: 10.18653/v1/W19-5301. URL <https://aclanthology.org/W19-5301/>.

Bengio, Y., Minderhann, S., Privitera, D., Besiroglu, T., Bommasani, R., Casper, S., Choi, Y., Fox, P., Garfinkel, B., Goldfarb, D., et al. International ai safety report. *arXiv preprint arXiv:2501.17805*, 2025.

Boroujeny, M. K., Jiang, Y., Zeng, K., and Mark, B. Multi-bit distortion-free watermarking for large language models. *arXiv preprint arXiv:2402.16578*, 2024.

Chao, P., Sun, Y., Dobriban, E., and Hassani, H. Watermarking language models with error correcting codes. *arXiv preprint arXiv:2406.10281*, 2024.

Chen, M. Evaluating large language models trained on code. *arXiv preprint arXiv:2107.03374*, 2021.

Chen, R., Wu, Y., Guo, J., and Huang, H. Improved unbiased watermark for large language models. In Che, W., Nabende, J., Shutova, E., and Pilehvar, M. T. (eds.), *Proceedings of the 63rd Annual Meeting of the Association for Computational Linguistics (Volume 1: Long Papers)*, pp. 20587–20601, Vienna, Austria, July 2025. Association for Computational Linguistics. ISBN 979-8-89176-251-0. doi: 10.18653/v1/2025.acl-long.1005. URL <https://aclanthology.org/2025.acl-long.1005/>.

Chiang, W.-L., Li, Z., Lin, Z., Sheng, Y., Wu, Z., Zhang, H., Zheng, L., Zhuang, S., Zhuang, Y., Gonzalez, J. E., Stoica, I., and Xing, E. P. Vicuna: An open-source chatbot impressing gpt-4 with 90%\* chatgpt quality, March 2023. URL <https://lmsys.org/blog/2023-03-30-vicuna/>.

Cobbe, K., Kosaraju, V., Bavarian, M., Chen, M., Jun, H., Kaiser, L., Plappert, M., Tworek, J., Hilton, J., Nakano, R., et al. Training verifiers to solve math word problems. *arXiv preprint arXiv:2110.14168*, 2021.

Cohen, A., Hoover, A., and Schoenbach, G. Watermarking language models for many adaptive users. In *2025 IEEE Symposium on Security and Privacy (SP)*, pp. 2583–2601. IEEE, 2025.

Comanici, G., Bieber, E., Schaekermann, M., Pasupat, I., Sachdeva, N., Dhillon, I., Blstein, M., Ram, O., Zhang, D., Rosen, E., et al. Gemini 2.5: Pushing the frontier with advanced reasoning, multimodality, long context, and next generation agentic capabilities. *arXiv preprint arXiv:2507.06261*, 2025.

Dathathri, S., See, A., Ghaisas, S., Huang, P.-S., McAdam, R., Welbl, J., Bachani, V., Kaskasoli, A., Stanforth, R., Matejovicova, T., et al. Scalable watermarking for identifying large language model outputs. *Nature*, 634(8035): 818–823, 2024.

Devlin, J., Chang, M.-W., Lee, K., and Toutanova, K. BERT: Pre-training of deep bidirectional transformers for language understanding. In Burstein, J., Doran, C., and Solorio, T. (eds.), *Proceedings of the 2019 Conference of the North American Chapter of the Association for Computational Linguistics: Human Language Technologies, Volume 1 (Long and Short Papers)*, pp. 4171–4186, Minneapolis, Minnesota, June 2019. Association for Computational Linguistics. doi: 10.18653/v1/N19-1423. URL <https://aclanthology.org/N19-1423/>.

Fairoze, J., Garg, S., Jha, S., Mahloujifar, S., Mahmoody, M., and Wang, M. Publicly-detectable watermarking for language models. *arXiv preprint arXiv:2310.18491*, 2023.

Fan, A., Jernite, Y., Perez, E., Grangier, D., Weston, J., and Auli, M. ELI5: Long form question answering. In Korhonen, A., Traum, D., and Màrquez, L. (eds.), *Proceedings of the 57th Annual Meeting of the Association for Computational Linguistics*, pp. 3558–3567, Florence, Italy, July 2019. Association for Computational Linguistics. doi: 10.18653/v1/P19-1346. URL <https://aclanthology.org/P19-1346/>.

Feng, X., Zhang, H., Zhang, Y., Zhang, L. Y., and Pan, S. Bimark: Unbiased multilayer watermarking for large language models. In *Forty-second International Conference on Machine Learning*, 2025. URL <https://openreview.net/forum?id=Zvyb3WAg03>.

Fernandez, P., Chaffin, A., Tit, K., Chappelier, V., and Furou, T. Three bricks to consolidate watermarks for large language models. In *2023 IEEE international workshop on information forensics and security (WIFS)*, pp. 1–6. IEEE, 2023.

Fu, J., Zhao, X., Yang, R., Zhang, Y., Chen, J., and Xiao, Y. GumbelSoft: Diversified language model watermarking via the GumbelMax-trick. In Ku, L.-W., Martins, A., and Srikumar, V. (eds.), *Proceedings of the 62nd Annual Meeting of the Association for Computational Linguistics (Volume 1: Long Papers)*, pp. 5791–5808, Bangkok, Thailand, August 2024. Association for Computational Linguistics. doi: 10.18653/v1/2024.acl-long.315. URL <https://aclanthology.org/2024.acl-long.315/>.

Goldreich, O., Goldwasser, S., and Micali, S. How to construct random functions. *Journal of the ACM (JACM)*, 33(4):792–807, 1986.

Grattafiori, A., Dubey, A., Jauhri, A., Pandey, A., Kadian, A., Al-Dahle, A., Letman, A., Mathur, A., Schelten, A., Vaughan, A., et al. The llama 3 herd of models. *arXiv preprint arXiv:2407.21783*, 2024.

Guo, D., Yang, D., Zhang, H., Song, J., Zhang, R., Xu, R., Zhu, Q., Ma, S., Wang, P., Bi, X., et al. Deepseek-r1: Incentivizing reasoning capability in llms via reinforcement learning. *arXiv preprint arXiv:2501.12948*, 2025.

Hamming, R. W. Error detecting and error correcting codes. *The Bell system technical journal*, 29(2):147–160, 1950.

Hermann, K. M., Kočiský, T., Grefenstette, E., Espeholt, L., Kay, W., Suleyman, M., and Blunsom, P. Teaching machines to read and comprehend. *Advances in neural information processing systems*, 28, 2015.

Hou, A., Zhang, J., He, T., Wang, Y., Chuang, Y.-S., Wang, H., Shen, L., Van Durme, B., Khashabi, D., and Tsvetkov, Y. SemStamp: A semantic watermark with paraphrastic robustness for text generation. In Duh, K., Gomez, H., and Bethard, S. (eds.), *Proceedings of the 2024 Conference of the North American Chapter of the Association for Computational Linguistics: Human Language Technologies (Volume 1: Long Papers)*, pp. 4067–4082, Mexico City, Mexico, June 2024a. Association for Computational Linguistics. doi: 10.18653/v1/2024.nacl-long.226. URL <https://aclanthology.org/2024.nacl-long.226/>.

Hou, A., Zhang, J., Wang, Y., Khashabi, D., and He, T. k-SemStamp: A clustering-based semantic watermark for detection of machine-generated text. In Ku, L.-W., Martins, A., and Srikumar, V. (eds.), *Findings of the Association for Computational Linguistics: ACL 2024*, pp. 1706–1715, Bangkok, Thailand, August 2024b. Association for Computational Linguistics. doi: 10.18653/v1/2024.findings-acl.98. URL <https://aclanthology.org/2024.findings-acl.98/>.

Hu, Z., Chen, L., Wu, X., Wu, Y., Zhang, H., and Huang, H. Unbiased watermark for large language models. *arXiv preprint arXiv:2310.10669*, 2023.

Jiang, H., Wang, X., Yi, P., Lei, S., and Lin, Y. Credid: Credible multi-bit watermark for large language models identification, 2025a. URL <https://arxiv.org/abs/2412.03107>.

Jiang, Y., Wu, C., Boroujeny, M. K., Mark, B., and Zeng, K. StealthInk: A multi-bit and stealthy watermark for large language models. In Singh, A., Fazel, M., Hsu, D., Lacoste-Julien, S., Berkenkamp, F., Maharaj, T., Wagstaff, K., and Zhu, J. (eds.), *Proceedings of the 42nd International Conference on Machine Learning*, volume 267 of *Proceedings of Machine Learning Research*, pp. 27685–27709. PMLR, 13–19 Jul 2025b. URL <https://proceedings.mlr.press/v267/jiang25j.html>.

Kirchenbauer, J., Geiping, J., Wen, Y., Katz, J., Miers, I., and Goldstein, T. A watermark for large language models. In Krause, A., Brunskill, E., Cho, K., Engelhardt, B., Sabato, S., and Scarlett, J. (eds.), *Proceedings of the 40th International Conference on Machine Learning*, volume 202 of *Proceedings of Machine Learning Research*, pp. 17061–17084. PMLR, 23–29 Jul 2023. URL <https://proceedings.mlr.press/v202/kirchenbauer23a.html>.

Kirchenbauer, J., Geiping, J., Wen, Y., Shu, M., Saifullah, K., Kong, K., Fernando, K., Saha, A., Goldblum, M., and Goldstein, T. On the reliability of watermarks for large language models. In *The Twelfth International Conference on Learning Representations*, 2024. URL <https://openreview.net/forum?id=DEJIDCmW0z>.

Krishna, K., Song, Y., Karpinska, M., Wieting, J., and Iyyer, M. Paraphrasing evades detectors of ai-generated text, but retrieval is an effective defense. *Advances in Neural Information Processing Systems*, 36:27469–27500, 2023.

Lau, G. K. R., Niu, X., Dao, H., Chen, J., Foo, C.-S., and Low, B. K. H. Waterfall: Scalable framework for robust text watermarking and provenance for LLMs. In Al-Onaizan, Y., Bansal, M., and Chen, Y.-N. (eds.), *Proceedings of the 2024 Conference on Empirical Methods in Natural Language Processing*, pp. 20432–20466, Miami, Florida, USA, November 2024. Association for Computational Linguistics. doi: 10.18653/v1/2024.emnlp-main.1138. URL <https://aclanthology.org/2024.emnlp-main.1138/>.

Lee, T., Hong, S., Ahn, J., Hong, I., Lee, H., Yun, S., Shin, J., and Kim, G. Who wrote this code? watermarking for code generation. In Ku, L.-W., Martins, A., and Srikumar, V. (eds.), *Proceedings of the 62nd Annual Meeting of the Association for Computational Linguistics (Volume 1: Long Papers)*, pp. 4890–4911, Bangkok, Thailand, August 2024. Association for Computational Linguistics. doi: 10.18653/v1/2024.acl-long.268. URL <https://aclanthology.org/2024.acl-long.268/>.

Li, B., Fu, Z., Zhang, M., Zhang, P., Sun, J., and Wang, X. Efficient and universal watermarking for llm-generated code detection, 2025. URL <https://arxiv.org/abs/2402.07518>.

Lin, C.-Y. Rouge: A package for automatic evaluation of summaries. In *Text summarization branches out*, pp. 74–81, 2004.

Liu, A., Pan, L., Hu, X., Meng, S., and Wen, L. A semantic invariant robust watermark for large language models. In *The Twelfth International Conference on Learning Representations*, 2024a. URL <https://openreview.net/forum?id=6p81pe4MNF>.

Liu, A., Pan, L., Lu, Y., Li, J., Hu, X., Zhang, X., Wen, L., King, I., Xiong, H., and Yu, P. A survey of text watermarking in the era of large language models. *ACM Computing Surveys*, 57(2):1–36, 2024b.

Liu, A. H., Khandelwal, K., Subramanian, S., Jouault, V., Rastogi, A., Sadé, A., Jeffares, A., Jiang, A., Cahill, A., Gavaudan, A., et al. Ministral 3. *arXiv preprint arXiv:2601.08584*, 2026.

Lu, Y., Liu, A., Yu, D., Li, J., and King, I. An entropy-based text watermarking detection method. In Ku, L.-W., Martins, A., and Srikumar, V. (eds.), *Proceedings of the 62nd Annual Meeting of the Association for Computational Linguistics (Volume 1: Long Papers)*, pp. 11724–11735, Bangkok, Thailand, August 2024. Association for Computational Linguistics. doi: 10.18653/v1/2024.acl-long.630. URL <https://aclanthology.org/2024.acl-long.630/>.

Luo, J., Zhang, W., Yuan, Y., Zhao, Y., Yang, J., Gu, Y., Wu, B., Chen, B., Qiao, Z., Long, Q., et al. Large language model agent: A survey on methodology, applications and challenges. *arXiv preprint arXiv:2503.21460*, 2025.

Merity, S., Xiong, C., Bradbury, J., and Socher, R. Pointer sentinel mixture models. *arXiv preprint arXiv:1609.07843*, 2016.

Miller, G. A. Wordnet: a lexical database for english. *Communications of the ACM*, 38(11):39–41, 1995.

Mitchell, E., Lee, Y., Khazatsky, A., Manning, C. D., and Finn, C. Detectgpt: Zero-shot machine-generated text detection using probability curvature. In *International conference on machine learning*, pp. 24950–24962. PMLR, 2023.

Papineni, K., Roukos, S., Ward, T., and Zhu, W.-J. Bleu: a method for automatic evaluation of machine translation. In *Proceedings of the 40th annual meeting of the Association for Computational Linguistics*, pp. 311–318, 2002.

Qu, W., Zheng, W., Tao, T., Yin, D., Jiang, Y., Tian, Z., Zou, W., Jia, J., and Zhang, J. Provably robust multi-bit watermarking for {AI-generated} text. In *34th USENIX Security Symposium (USENIX Security 25)*, pp. 201–220, 2025.

Raffel, C., Shazeer, N., Roberts, A., Lee, K., Narang, S., Matena, M., Zhou, Y., Li, W., and Liu, P. J. Exploring the limits of transfer learning with a unified text-to-text transformer. *Journal of machine learning research*, 21(140):1–67, 2020.

Reimers, N. and Gurevych, I. Sentence-BERT: Sentence embeddings using Siamese BERT-networks. In Inui, K., Jiang, J., Ng, V., and Wan, X. (eds.), *Proceedings of the 2019 Conference on Empirical Methods in Natural Language Processing and the 9th International Joint Conference on Natural Language Processing (EMNLP-IJCNLP)*, pp. 3982–3992, Hong Kong, China, November 2019. Association for Computational Linguistics. doi: 10.18653/v1/D19-1410. URL <https://aclanthology.org/D19-1410/>.

Ren, Y., Guo, P., Cao, Y., and Ma, W. Subtle signatures, strong shields: Advancing robust and imperceptible watermarking in large language models. In Ku, L.-W., Martins, A., and Srikumar, V. (eds.), *Findings of the Association for Computational Linguistics: ACL 2024*, pp. 5508–5519, Bangkok, Thailand, August 2024. Association

for Computational Linguistics. doi: 10.18653/v1/2024.327. URL <https://aclanthology.org/2024.findings-acl.327/>.

Tang, R., Chuang, Y.-N., and Hu, X. The science of detecting llm-generated text. *Communications of the ACM*, 67(4):50–59, 2024.

Team, G., Riviere, M., Pathak, S., Sessa, P. G., Hardin, C., Bhupatiraju, S., Husseinot, L., Mesnard, T., Shahriari, B., Ramé, A., et al. Gemma 2: Improving open language models at a practical size. *arXiv preprint arXiv:2408.00118*, 2024.

Tu, S., Sun, Y., Bai, Y., Yu, J., Hou, L., and Li, J. WaterBench: Towards holistic evaluation of watermarks for large language models. In Ku, L.-W., Martins, A., and Srikumar, V. (eds.), *Proceedings of the 62nd Annual Meeting of the Association for Computational Linguistics (Volume 1: Long Papers)*, pp. 1517–1542, Bangkok, Thailand, August 2024. Association for Computational Linguistics. doi: 10.18653/v1/2024.acl-long.83. URL <https://aclanthology.org/2024.acl-long.83/>.

Vaswani, A., Shazeer, N., Parmar, N., Uszkoreit, J., Jones, L., Gomez, A. N., Kaiser, Ł., and Polosukhin, I. Attention is all you need. *Advances in neural information processing systems*, 30, 2017.

Wang, L., Yang, W., Chen, D., Zhou, H., Lin, Y., Meng, F., Zhou, J., and Sun, X. Towards codable watermarking for injecting multi-bits information to LLMs. In *The Twelfth International Conference on Learning Representations*, 2024. URL <https://openreview.net/forum?id=JYu5F1qm9D>.

Wang, Y., Ren, Y., Cao, Y., and Fang, B. From trade-off to synergy: A versatile symbiotic watermarking framework for large language models. In Che, W., Nabende, J., Shutova, E., and Pilehvar, M. T. (eds.), *Proceedings of the 63rd Annual Meeting of the Association for Computational Linguistics (Volume 1: Long Papers)*, pp. 10306–10322, Vienna, Austria, July 2025. Association for Computational Linguistics. ISBN 979-8-89176-251-0. doi: 10.18653/v1/2025.acl-long.509. URL <https://aclanthology.org/2025.acl-long.509/>.

Wu, Y., Hu, Z., Zhang, H., and Huang, H. Dipmark: A stealthy, efficient and resilient watermark for large language models. 2023.

Xu, X., Jia, J., Yao, Y., Liu, Y., and Li, H. Robust multi-bit text watermark with LLM-based paraphrasers. In *Forty-second International Conference on Machine Learning*, 2025. URL <https://openreview.net/forum?id=DVjklng5x>.

Yoo, K., Ahn, W., and Kwak, N. Advancing beyond identification: Multi-bit watermark for large language models. In Duh, K., Gomez, H., and Bethard, S. (eds.), *Proceedings of the 2024 Conference of the North American Chapter of the Association for Computational Linguistics: Human Language Technologies (Volume 1: Long Papers)*, pp. 4031–4055, Mexico City, Mexico, June 2024. Association for Computational Linguistics. doi: 10.18653/v1/2024.naacl-long.224. URL <https://aclanthology.org/2024.naacl-long.224/>.

Yu, Z., Jiang, X., Gu, W., Wang, Y., Wen, Q., Zhang, S., and Ye, W. SAEMark: Steering personalized multilingual LLM watermarks with sparse autoencoders. In *The Thirty-ninth Annual Conference on Neural Information Processing Systems*, 2025. URL <https://openreview.net/forum?id=tXnyVPNOfa>.

Zamir, O. Excuse me, sir? your language model is leaking (information). *arXiv preprint arXiv:2401.10360*, 2024.

Zhang, R., Hussain, S. S., Neekhara, P., and Koushanfar, F. {REMARK-LLM}: A robust and efficient watermarking framework for generative large language models. In *33rd USENIX Security Symposium (USENIX Security 24)*, pp. 1813–1830, 2024.

Zhao, X., Ananth, P. V., Li, L., and Wang, Y.-X. Provable robust watermarking for AI-generated text. In *The Twelfth International Conference on Learning Representations*, 2024. URL <https://openreview.net/forum?id=SsmT8aO45L>.

Zheng, L., Chiang, W.-L., Sheng, Y., Zhuang, S., Wu, Z., Zhuang, Y., Lin, Z., Li, Z., Li, D., Xing, E., et al. Judging llm-as-a-judge with mt-bench and chatbot arena. *Advances in neural information processing systems*, 36: 46595–46623, 2023.

## A. Related Work

Existing LLM watermarking methods can be broadly categorized into zero-bit watermarking and multi-bit watermarking approaches (Liu et al., 2024b), depending on whether message bits are explicitly embedded.

### A.1. Zero-bit Watermarking

The pioneering KGW method (Kirchenbauer et al., 2023) first introduced token-level watermarking by partitioning the vocabulary into "green" and "red" token lists and modifying the logits distribution during inference to embed a watermark signal. To enhance robustness, Unigram (Zhao et al., 2024) adopted a globally fixed vocabulary partition, while subsequent works (Liu et al., 2024a; Ren et al., 2024; Hou et al., 2024b;a) leveraged semantic and frequency-based features to defend against editing attacks. To mitigate text quality degradation, several studies proposed entropy-based watermarking schemes (Lu et al., 2024; Lee et al., 2024; Wang et al., 2025), while others explored unbiased reweighting strategies (Wu et al., 2023; Hu et al., 2023; Chen et al., 2025). Additionally, Dathathri et al. (2024); Aaronson (2023); Fu et al. (2024) designed alternative token sampling mechanisms that preserve the original logits distribution. Overall, zero-bit watermarking can only determine whether a text contains a watermark, limited in broader scenarios such as content provenance tracing.

### A.2. Multi-bit Watermarking

Fernandez et al. (2023); Jiang et al. (2025a) embedded multi-bit message by establishing a mapping between predefined watermark keys and message bits. Wang et al. (2024); Cohen et al. (2025) divides both the text and message into multiple independent blocks, sequentially encoding each message segment into a corresponding text block. Although these methods achieve moderate decoding accuracy, they require enumerating all candidate messages during decoding, resulting in high exponential computational complexity with respect to message length (i.e.,  $O(2^b)$  for  $b$  bits). To overcome this limitation, Zhang et al. (2024); Xu et al. (2025); Lau et al. (2024) explore training-based and post-hoc approaches, while Yu et al. (2025) propose a black-box method for generating sentence-level watermarks. In contrast, MPAC (Yoo et al., 2024) assigns distinct message bits to different tokens via hash functions and extends the KGW framework accordingly. Building upon this idea, BiMark (Feng et al., 2025) and StealthInk (Jiang et al., 2025b), Zamir (2024); Boroujeny et al. (2024) developed distortion-free multi-bit watermark variants, while Qu et al. (2025) introduced error-correcting codes (Chao et al., 2024; Fairoze et al., 2023; Li et al., 2025) to further enhance decoding robustness. Despite these advances, current multi-bit watermarking techniques still struggle to jointly optimize capacity, decoding accuracy, efficiency, and text quality.

Table 3. The comparison between **WorldCup** (our method) and related studies, categorized as yes (✓), partial (P), or no (✗).

Multi-bit Watermarking	Detectability	Text Quality	Robustness	Token Capacity	Accuracy	Efficiency
MPAC (Yoo et al., 2024)	✓	P	✗	✓	✓	✓
BiMark (Feng et al., 2025)	✓	✓	P	P	✓	✓
SegMark (Qu et al., 2025)	✓	P	✓	✓	✓	✗
StealthInk (Jiang et al., 2025b)	✓	✓	✗	✓	P	✓
<b>WorldCup (Ours)</b>	✓	✓	✓	✓	✓	✓

## B. Baselines

For each baseline, we follow the configurations in original papers. The key hyperparameter settings are as follows:

- **BiMark** (Feng et al., 2025): The base scaling factor  $\tilde{\delta}$  is set to 1.0, and the number of layers  $d$  is 10. The proportion  $\gamma$  of green lists is 0.5 and the window size is 2. The values of  $c\_key$  and  $bit\_idx\_key$  are 530773 and 283519, respectively.
- **MPAC** (Yoo et al., 2024): We adopt the lefthash scheme. The window size is 2, and the proportion  $\gamma$  of green lists is 0.5. A bias  $\delta = 2.0$  is added to the logit scores of green tokens. The hash key is 15485863.
- **SegMark** (Qu et al., 2025): We use the RSBH scheme (balanced segment assignment with ECC). The window size is 2, the proportion  $\gamma$  of green lists is 0.5, and a bias  $\delta = 2.0$  is added to the logit of green tokens. The salt key is 35317.

## C. Datasets

We follow previous work (Tu et al., 2024) to evaluate our multi-bit watermark method on the following datasets:

- **C4** (Raffel et al., 2020) dataset is a large-scale, high-quality English pretraining corpus constructed by Google from Common Crawl. After extensive cleaning and filtering to remove non-linguistic, low-quality, and duplicate content, it yields roughly 750 GB of clean English text. We use the processed version in <https://huggingface.co/datasets/allenai/c4>.
- **OpenGen** (Krishna et al., 2023) dataset contains 3,000 two-sentence text blocks drawn from the validation split of WikiText-103 (Merity et al., 2016), with the subsequent 300 tokens written by human. We sample 200 instances from this dataset for our experiments. The dataset are in <https://github.com/XuandongZhao/Unigram-Watermark>.
- **WMT** (Barrault et al., 2019) dataset is a widely recognized benchmark in machine translation, containing parallel corpora from diverse sources and covering multiple language pairs. For our downstream evaluation, we primarily collect 200 samples from the WMT’19 De-En subset, with decoding parameters set to `max_new_tokens = 64` and `min_new_tokens = 16` (**short input, short output**). We embed **2-bit** message into each generated sample. It can be found at the following link: <https://huggingface.co/datasets/wmt/wmt19/viewer/de-en/validation>.
- **CNN\_DailyMail** (Hermann et al., 2015) dataset is a large-scale English news corpus containing over 300,000 unique articles written by journalists from CNN and the Daily Mail. The current release supports both extractive and abstractive summarization. We collect 200 samples and prompt the model to produce a one-sentence summary, with `max_new_tokens = 64` and `min_new_tokens = 32` (**long input, short output**), and embed a **16-bit** message into each generated summary. Details of the dataset can be found at: [https://huggingface.co/datasets/abisee/cnn\\_dailymail](https://huggingface.co/datasets/abisee/cnn_dailymail).
- **ELI5** (Fan et al., 2019) dataset is a long-form QA dataset sourced from the Reddit community “Explain Like I’m Five.” It contains 270k diverse questions that require multi-sentence, explanatory answers supported by web evidence. We get 200 data points and set `max_new_tokens = 256` and `min_new_tokens = 64` (**short input, long output**), and embed a **32-bit** message into each generated answer. We use the processed subset available at [https://github.com/THU-KEG/WaterBench/blob/main/data/WaterBench/2-1\\_longform\\_qa.jsonl](https://github.com/THU-KEG/WaterBench/blob/main/data/WaterBench/2-1_longform_qa.jsonl).
- **GSM8K** (Cobbe et al., 2021) dataset consists of 8,500 high-quality grade-school math word problems requiring 2–8 steps of reasoning, with answers expressed in natural language. For downstream evaluation, we sample 200 instances and use an 8-shot setting with `max_new_tokens = 256` and `min_new_tokens = 64` (**long input, long output**), and embed a **4-bit** message into each generated solution. The dataset is available at: <https://huggingface.co/datasets/openai/gsm8k>.

## D. Metrics

All evaluation metrics used in our experiments are described in detail below:

- **Bit Accuracy (Bit Acc.)** measures the proportion of correctly extracted bits across all samples. Let  $\mathbf{m}^{(j)} = (m_1^{(j)}, \dots, m_L^{(j)})$  denote the embedded message of length  $L$  for the  $j$ -th sample, and  $\hat{\mathbf{m}}^{(j)} = (\hat{m}_1^{(j)}, \dots, \hat{m}_L^{(j)})$  be the corresponding extracted message. The Bit Accuracy over  $n$  samples is defined as

$$\text{Bit Acc.} = \frac{1}{nL} \sum_{j=1}^n \sum_{i=1}^L \mathbb{I}[\hat{m}_i^{(j)} = m_i^{(j)}] \quad (8)$$

where  $\mathbb{I}[\cdot]$  denotes the indicator function. It reflects fine-grained bit-level decoding performance, as shown in Table 1.

- **Message Extracted Rate (ME Rate)** quantifies the probability of perfectly recovering the entire embedded message. A message is considered successfully extracted if and only if all its bits are correctly recovered. Formally, the Message Extracted Rate over  $n$  samples is defined as:

$$\text{ME Rate} = \frac{1}{n} \sum_{j=1}^n \mathbb{I}[\hat{\mathbf{m}}^{(j)} = \mathbf{m}^{(j)}]. \quad (9)$$

It is a strict metric that penalizes any bit error and reflects end-to-end message recovery reliability, as shown in Table 4.

- **F1 Score** is the harmonic mean of precision and recall:

$$F1 = 2 \cdot \frac{\text{Precision} \cdot \text{Recall}}{\text{Precision} + \text{Recall}} \quad (10)$$

**Best F1 Score** denotes the maximum F1 score obtained over a threshold sweep, commonly used for evaluating binary classifiers without fixing a specific decision threshold.

- **AUROC Curve** (Receiver Operating Characteristic) plots **TPR** (True Positive Rate) against **FPR** (False Positive Rate) under varying decision thresholds. The area under this curve (**AUC**) summarizes the watermark detector’s ranking ability, with values closer to 1 indicating stronger discriminative performance.
- **Perplexity (PPL)** measures how well a language model predicts a given text. For a sequence  $x_{1:T}$ :

$$PPL = \exp\left(-\frac{1}{T} \sum_{t=1}^T \log p(x_t \mid x_{<t})\right) \quad (11)$$

Lower perplexity implies more confident and accurate language modeling. We report median PPL rather than mean PPL, as it provides more stable estimates and is less sensitive to extreme values (Jiang et al., 2025b).

- **BLEU** (Papineni et al., 2002) (Bilingual Evaluation Understudy) is a standard automatic metric that quantifies lexical similarity by computing n-gram precision between machine-generated translations and human reference texts, with a brevity penalty to discourage overly short outputs.
- **Pass@K** (Chen, 2021) measures the probability that at least one of the k generated solutions is correct. In this work, we follow the standard setting and report the results of GSM8K dataset using **Pass@1**.
- **Cosine similarity** Cosine similarity computes the cosine of the angle between two vectors to measure their semantic similarity. We use Sentence-BERT (Reimers & Gurevych, 2019) to obtain sentence embeddings and apply cosine similarity to quantify the semantic closeness of natural texts and AI-generated texts.
- **ROUGE Score** (Lin, 2004) measures overlap between generated and reference text. Among its variants, we use ROUGE-L, which computes the longest common subsequence (LCS) between the candidate and reference, capturing sentence-level structural similarity beyond contiguous n-gram overlap.
- **Log Diversity** quantifies textual diversity by measuring n-gram uniqueness. For each n-gram length  $n \in \{2, 3, 4\}$ , we compute a diversity score and aggregate them by taking the product of the three adjusted scores:

$$\text{LogDiversity} = -\log \left( \max \left( 1 - \prod_{n \in \{2,3,4\}} \left( 1 - \left( 1 - \frac{\text{unique}_n}{\text{total}_n} \right) / 100 \right), e^{-20} \right) \right) \quad (12)$$

This log transformation stabilizes the metric and yields higher scores for more diverse, less repetitive text.

- **GPT4 Score** (Zheng et al., 2023) leverages GPT-4 (Achiam et al., 2023) as an evaluator. The model is prompted to rate the quality, correctness, or faithfulness of generated text relative to a reference or specification. This human-aligned evaluation correlates closely with expert judgments. The scoring template we use is as follows:

**GPT-4 Judge Template**

You are an strict text quality evaluator. Your task is to compare a candidate text against a reference text (which serves as the ground truth) and produce a single final quality score.

Evaluation Criteria:

1. Fluency (Naturalness): How natural, grammatical, and readable the candidate text is.
2. Adequacy: How well the candidate preserves the meaning of the reference.
3. Coherence: How logically consistent and well-structured the candidate text is.
4. Relevance: How well the content matches the intent and key information of the reference.
5. Style Consistency: How closely the candidate matches the tone and style of the reference.

Scoring:

- For each criterion, assign a score from 1 to 10.
- Compute the final score as the average of all criterion scores.
- Output ONLY the final numerical score (e.g., 3.8). Do not explain, justify, or output intermediate scores.

Reference Text: xxx Candidate Text: xxx Score:

## E. Backbone Models

We primarily employ the following backbone models in our experiments:

- **LLaMA3** family (Grattafiori et al., 2024) is developed by Meta, built upon an optimized Transformer architecture, which includes both pre-trained and instruction-tuned generative text models with sizes of 8B and 70B parameters. Both the 8B and 70B variants adopt Grouped Query Attention (GQA) to improve inference scalability. In this paper, we use the LLaMA3-8B Base and LLaMA3.1-8B-Instruct version, as details can be found in <https://huggingface.co/collections/meta-llama/meta-llama-3>.
- **Gemma2** family (Team et al., 2024) is a series of lightweight open-source models released by Google, developed using the same research foundations and technologies as the Gemini models. These models are text-to-text, decoder-only LLMs that currently support English, and are suitable for a wide range of text generation tasks. In this paper, we mainly use the Gemma2-9B-Base and Gemma2-9B-Instruct version, as details can be found in <https://huggingface.co/google/gemma-2-9b>.
- **Minstral** family (Liu et al., 2026) belongs to Mistral AI's latest third-generation models released in 2025, which includes three state-of-the-art small, dense models (3B, 8B, and 14B). These models support applications that understand text, images, and logic across 40+ languages, and can be used for coding, collaboration, or document analysis. In this paper, we utilize the Minstral-8B-Instruct, as detailed can be found in <https://huggingface.co/mistralai/Minstral-8B-Instruct-2410>.

## F. Attack Settings

To evaluate the robustness of the watermark, we design the following various attack scenarios:

- **Word-D (ratio =  $\rho$ )**: Randomly deletes a proportion  $\rho$  of words from the watermarked text.
- **Word-S-Dict (ratio =  $\rho$ )**: Randomly replaces a proportion  $\rho$  of words with their synonyms based on the WordNet (Miller, 1995) lexical dictionary.
- **Word-S-BERT (ratio =  $\rho$ )**: Randomly substitutes a proportion  $\rho$  of words with context-aware synonyms generated by a BERT-based (Devlin et al., 2019) model.
- **Copy-Paste ( $n - \rho$ )**: Randomly splits the watermarked text into  $n$  segments and inserts them into non-watermarked text, such that the inserted non-watermarked content accounts for a total proportion  $\rho$ .
- **Translation (en-zh)**: Translates the watermarked text from English to Chinese and then back to English using a fine-tuned T5 translation model: [https://huggingface.co/utrobinmv/t5\\_translate\\_en\\_ru\\_zh\\_small\\_1024](https://huggingface.co/utrobinmv/t5_translate_en_ru_zh_small_1024).

- **Rephrase (GPT-4o):** Rewrites the watermarked text using the GPT-4o API with the temperature set to 0.7.
- **Rephrase (DIPPER-1):** Rephrases the text using the DIPPER model with controlled lexical diversity and word order diversity (lex\_diversity= $\rho_1$  order\_diversity= $\rho_2$ , max\_new\_tokens=256, sent\_interval=1, top\_p=0.75).
- **Rephrase (DIPPER-2):** Rephrases the text using the DIPPER model under alternative settings of lexical and order diversity (lex\_diversity= $\rho'_1$  order\_diversity= $\rho'_2$ , max\_new\_tokens=256, sent\_interval=1, top\_p=0.75).

## G. Theoretical Results

### G.1. Proof of Proposition 3.5

**Proof.** Let the random variables  $G_0 = \mathbf{g}_0(\mathbf{x}, r)$  and  $G_1 = \mathbf{g}_1(\mathbf{x}, r)$  denote the  $g$ -values used to encode message bits 0 and 1, respectively. We assume that  $G_0$  and  $G_1$  share the same marginal distribution  $F_g$ , which ensures identical token-wise bias strength under both hypotheses.

**Step 1: Discriminability at the scoring level.** We first quantify the separation between the two encoding hypotheses at the scoring level by the expected squared difference:

$$D \triangleq \mathbb{E}[(G_1 - G_0)^2]. \quad (13)$$

Expanding this expression yields:

$$D = \mathbb{E}(G_1^2) + \mathbb{E}(G_0^2) - 2\mathbb{E}[G_1 G_0] \quad (14)$$

Let  $\mu_i = \mathbb{E}[G_i]$  and  $\sigma_i^2 = \text{Var}(G_i)$  for  $i \in 0, 1$ . Rewriting Eq. 14 in mean-variance form gives

$$D = \sigma_1^2 + \sigma_0^2 - 2\text{Cov}(G_1, G_0) + (\mu_1 - \mu_0)^2 \quad (15)$$

Under the identical-marginal assumption ( $\mu_0 = \mu_1 = \mu$ ,  $\sigma_0^2 = \sigma_1^2 = \sigma^2$ ), Eq. 15 simplifies to

$$D = 2\sigma^2 - 2\text{Cov}(G_1, G_0) \quad (16)$$

For fixed marginals,  $D$  is maximized by minimizing the covariance between  $G_0$  and  $G_1$ . By the Cauchy-Schwarz inequality:

$$\text{Cov}(G_1, G_0) \geq -\sqrt{\text{Var}(G_1) \text{Var}(G_0)} = -\sigma^2 \quad (17)$$

with equality if and only if  $G_1$  and  $G_0$  are perfectly anti-correlated. Substituting this bound into Eq. 16 yields:

$$D_{\max} = 2\sigma^2 - 2(-\sigma^2) = 4\sigma^2 \quad (18)$$

**Step 2: Consistency with equal-mean constraint.** Perfect anti-correlation implies  $G_1 = a - G_0$  almost surely. Enforcing  $\mathbb{E}[G_1] = \mathbb{E}[G_0] = \mu$  gives  $a = 2\mu$ , and hence:

$$G_1 = 2\mu - G_0. \quad (19)$$

Under the symmetric Bernoulli setting used in our experiments ( $\mu = 0.5$ ), this reduces to the complementary construction  $G_1 = 1 - G_0$ .

**Step 3: Implication for embedding distributions.** While the above analysis operates at the level of  $g$ -values, it has direct implications for the resulting embedding distributions induced by tournament sampling. Each tournament round selects the higher-scoring token according to the corresponding  $g$ -value function. Therefore, for any fixed candidate set, the probability that two encoding hypotheses produce different winners is a monotonically increasing function of the separation

between their underlying scores. In particular, perfect anti-correlation maximizes the probability that a token favored under  $G_0$  is disfavored under  $G_1$ , and vice versa. As a result, the induced token distributions under message bits 0 and 1 are pushed toward opposite extremes of the sampling decision boundary. This maximizes the distinguishability of the resulting embedding distributions in terms of any decision-based statistical distance (e.g., total variation or hypothesis-testing error).

Consequently, complementary  $g$ -values achieve the maximum possible discriminability between embedding distributions under the tournament sampling mechanism, completing the proof.

## G.2. Vectorized WorldCup Sampling

In the multi-bit WorldCup watermark, once a message bit is assigned to each token, the corresponding  $g$ -value function is uniquely determined. Consequently, conditioning on the assigned message bits, the generation of each token is distributionally equivalent to that of a zero-bit watermark. This observation allows us to directly adopt the analytical framework of SynthID (Dathathri et al., 2024).

Let  $p(\cdot)$  denote the base language-model distribution over the vocabulary  $V$ . For any token  $x_t$ , random seed  $r$ , and  $g$ -value function  $g_\ell(\cdot, r)$  at layer  $\ell$ , we define:

$$\begin{aligned} p(V^{=g_\ell(x_t, r)}) &:= \sum_{x \in \mathcal{V}: g_\ell(x, r) = g_\ell(x_t, r)} p(x), \\ p(V^{<g_\ell(x_t, r)}) &:= \sum_{x \in \mathcal{V}: g_\ell(x, r) < g_\ell(x_t, r)} p(x), \\ p(V^{\leq g_\ell(x_t, r)}) &:= \sum_{x \in \mathcal{V}: g_\ell(x, r) \leq g_\ell(x_t, r)} p(x). \end{aligned} \quad (20)$$

**Theorem G.1.** (Vectorized form, single-layer WorldCup sampling). *Given a probability distribution  $P_\Theta$  over  $\mathcal{V}$ , random seed  $r \in \mathcal{R}$ ,  $g$ -value distribution  $\mathbf{g}_0$  and  $\mathbf{g}_1$ , and the number of leaves  $N \geq 2$ , message  $\mathbf{m}$ , the watermarked distribution  $q(\cdot | P_\Theta, r_t, m, N, \mathbf{m}, p, \mathbf{g}_0, \mathbf{g}_1)$  for  $m = 1$  is given by:*

$$q(\cdot | P_\Theta, r_t, m, N, \mathbf{m}, p, \mathbf{g}_0, \mathbf{g}_1) = \begin{cases} p(x_t) \left( \frac{p(V^{\leq g(x_t, r)})^N - p(V^{< g(x_t, r)})^N}{p(V^{= g(x_t, r)})} \right) & \text{if } p(x_t) \neq 0 \\ 0 & \text{if } p(x_t) = 0 \end{cases} \quad (21)$$

where  $g = \mathbf{g}_0 = g_1^{(0)}$  if  $\mathbf{m}[p] = 0$  else  $g = \mathbf{g}_1 = g_1^{(1)}$  when  $m = 1$

**Proof.** We first note that if  $p(x_t) = 0$ , then  $\mathbb{P}(\text{Alg. 1 returns } x_t) = 0$ . Hence, we assume  $p(x_t) > 0$  in the following derivation. In a single-layer tournament,  $N$  samples participate in the selection. Let  $|Y^*| = j$  denote the number of tokens in the winning set, and suppose that  $x_t$  appears  $i$  times among these  $j$  tokens (pairwise comparison is not required). The probability that outputs  $x_t$  is:

$$\begin{aligned} \mathbb{P}(\text{Alg. 1 returns } x_t) &= \sum_{j=1}^N \sum_{i=1}^j \mathbb{P}(|Y^*| = j, x_t \text{ appears } i \text{ times in } Y^*, \text{Alg. 1 returns } x_t) \\ &= \sum_{j=1}^N \sum_{i=1}^j \binom{N}{j} p(V^{< g(x_t, r)})^{N-j} \binom{j}{i} p(x_t)^i p(V^{= g(x_t, r)} \setminus x_t)^{j-i} \frac{i}{j}. \end{aligned} \quad (22)$$

Rearranging the summations yields:

$$\mathbb{P}(\text{Alg. 1 returns } x_t) = \sum_{j=1}^N \binom{N}{j} p(V^{< g(x_t, r)})^{N-j} \sum_{i=1}^j \binom{j}{i} \frac{i}{j} p(x_t)^i p(V^{= g(x_t, r)} \setminus x_t)^{j-i}. \quad (23)$$

**Lemma G.2.**

$$\sum_{i=1}^j \binom{j}{i} \frac{i}{j} a^i b^{j-i} = a(a+b)^{j-1} \quad (24)$$

Using the identity G.2, and letting  $a = p(x_t)$  and  $b = p(V^{=g(x_t, r)} \setminus x_t)$ , we obtain:

$$\sum_{i=1}^j \binom{j}{i} \frac{i}{j} p(x_t)^i p(V^{=g(x_t, r)} \setminus x_t)^{j-i} = p(x_t) p(V^{=g(x_t, r)})^{j-1}. \quad (25)$$

Substituting back gives:

$$\begin{aligned} \mathbb{P}(\text{Alg. 1 returns } x_t) &= \sum_{j=1}^N \binom{N}{j} p(V^{<g(x_t, r)})^{N-j} p(x_t) p(V^{=g(x_t, r)})^{j-1} \\ &= \frac{p(x_t)}{p(V^{=g(x_t, r)})} \sum_{j=1}^N \binom{N}{j} p(V^{<g(x_t, r)})^{N-j} p(V^{=g(x_t, r)})^j. \end{aligned} \quad (26)$$

Applying the binomial theorem finally yields:

$$\mathbb{P}(\text{Alg. 1 returns } x_t) = \frac{p(x_t)}{p(V^{=g(x_t, r)})} \left( p(V^{\leq g(x_t, r)})^N - p(V^{<g(x_t, r)})^N \right). \quad (27)$$

In particular if  $N = 2$ , then:

$$\mathbb{P}(\text{Alg. 1 returns } x_t) = p(x_t) \left[ p(x_t) + 2p(V^{<g_1(x_t)}) \right] \quad (28)$$

When the  $g$ -value distribution  $\mathbf{g}$  is binary (i.e.,  $g \in \{0, 1\}$ ), the watermark distribution induced by a single-layer tournament with  $N$  candidates is given by

$$q(\cdot \mid P_\Theta, r_t, m, N, \mathbf{m}, p, \mathbf{g}_0, \mathbf{g}_1) = \begin{cases} p(x_t) p(V^{g=0})^{N-1}, & \text{if } g(x_t, r) = 0, \\ p(x_t) \frac{1 - p(V^{g=0})^N}{p(V^{g=1})}, & \text{if } g(x_t, r) = 1, \end{cases} \quad (29)$$

where  $p(V^{g=0}) := \sum_{x \in V: g(x, r)=0} p(x)$  and  $p(V^{g=1}) := \sum_{x \in V: g(x, r)=1} p(x)$ .

By a straightforward induction on the number of layers, the above result extends directly to the  $m$ -layer WorldCup sampling:

**Theorem G.3. (Vectorized form, multi-layer WorldCup sampling).** *Given a single-layer WorldCup sampling distribution  $q(P_\Theta, g(\cdot), N)$ :*

$$\begin{aligned} q^{(1)}(\cdot) &:= q(\cdot \mid P_\Theta, r_t, m, N, \mathbf{m}, p, \mathbf{g}_0, \mathbf{g}_1) \\ q^{(2)}(\cdot) &:= q(\cdot \mid q^{(1)}, r_t, m, N, \mathbf{m}, p, \mathbf{g}_0, \mathbf{g}_1) \\ &\dots \\ q^{(m)}(\cdot) &:= q(\cdot \mid q^{(m-1)}, r_t, m, N, \mathbf{m}, p, \mathbf{g}_0, \mathbf{g}_1) \end{aligned} \quad (30)$$

It follows that  $q^{(m)}(\cdot)$  is equal to the  $m$ -layer WorldCup watermarked distribution  $q(\cdot \mid \text{Alg. 1 return } x_t)$

**Proof.** The above theorem follows straightforwardly by induction on  $m$ . The case  $m = 1$  is ensured by Theorem G.1. Assume that the statement holds for  $m - 1$ . For an  $m$ -layer tournament, we may equivalently first execute  $N$ -many  $(m - 1)$ -layer tournaments and then apply a single-layer tournament to the resulting winners via  $g_m(\cdot, r)$ . By the induction assumption, the  $N$  winners are drawn from  $q^{(m-1)}(\cdot)$  as defined in Eq. 30, and by Theorem G.1 the winner of the single-layer tournament is given by  $q(\cdot \mid q^{(m-1)}, r_t, m, N, \mathbf{m}, p, \mathbf{g}_0, \mathbf{g}_1)$ .

### G.3. $k$ -bit WorldCup Watermarking

We can naturally extend Equation 5 to  $k > 2$  bits. Let  $\mathbf{m}' \in \{0, 1\}^k$  denote a  $k$ -bit message, and let  $\{q_0, q_1, \dots, q_{k-1}\}$  be the corresponding  $g$ -value functions  $g_i$  or probability subsets associated with each bit. Then, the unnormalized watermark distribution for a message  $\mathbf{m}'$  can be written as:

$$P_{\Theta, \mathbf{m}'} = \sum_{i=0}^{k-1} (b_i \bar{q}_i + (1 - b_i) q_i) - \lambda \sum_{i=0}^{k-1} (b_i q_i + (1 - b_i) \bar{q}_i) \quad (31)$$

where  $b_i$  is the  $i$ -th bit of  $\mathbf{m}'$ , and  $\bar{q}_i$  is the distribution induced by the complementary  $g$ -value function  $\bar{g}_i$ .

### G.4. Compute Watermark Z-score

Let  $\mathbf{y} = (y_1, \dots, y_T)$  denote a generated text of length  $T$  produced by an  $m$ -layer WorldCup sampling scheme. As in multi-bit watermarking, each token  $y_t$  is deterministically mapped, via the shared hash function and watermarking key, to a message bit position  $p_t \in \{1, \dots, b\}$ . For each token  $y_t$  and layer  $\ell \in \{1, \dots, m\}$ , we evaluate complementary  $g$ -value functions  $g_\ell(y_t, r) \in \{0, 1\}$  and  $\bar{g}_\ell(y_t, r) = 1 - g_\ell(y_t, r)$ , and define the signed token–layer score:

$$d_{t, \ell} \triangleq g_\ell(y_t, r) - \bar{g}_\ell(y_t, r) = 2g_\ell(y_t, r) - 1 \quad (32)$$

Rather than aggregating all tokens simultaneously, we compute the detection statistic in a bit-wise, cumulative manner. Let  $\mathcal{T}_p = \{t : p_t = p\}$  denote the set of tokens assigned to bit position  $p$ , and define the cumulative token set up to position  $p$  as  $\mathcal{C}_p = \bigcup_{i=1}^p \mathcal{T}_i$ . The confidence-aware statistic after incorporating the first  $p$  bit positions is defined as

$$S_p(\mathbf{y}) = \frac{1}{m|\mathcal{C}_p|} \sum_{t \in \mathcal{C}_p} \sum_{\ell=1}^m d_{t, \ell} \quad (33)$$

As  $p$  increases, token–layer contributions are progressively accumulated.

Under the null hypothesis  $H_0$  of unwatermarked text, the complementary  $g$ -value functions are symmetric and exchangeable, yielding  $\mathbb{E}_{H_0}[g_\ell(y_t, r)] = \mathbb{E}_{H_0}[\bar{g}_\ell(y_t, r)] = 0.5$ . Consequently,  $\mathbb{E}_{H_0}[d_{t, \ell}] = 0$  and thus  $\mathbb{E}_{H_0}[S_p(\mathbf{y})] = 0$  for all  $p$ . Moreover, since  $d_{t, \ell} \in \{-1, +1\}$  with equal probability under  $H_0$ , we have  $\text{Var}_{H_0}(d_{t, \ell}) = 1$ . Assuming approximate independence across token–layer pairs  $(t, \ell)$ , the variance of the cumulative statistic is  $\text{Var}_{H_0}(S_p(\mathbf{y})) = \frac{1}{m|\mathcal{C}_p|}$ .

We therefore define a position-dependent standardized detection statistic

$$z_p = \frac{S_p(\mathbf{y})}{\sqrt{1/(m|\mathcal{C}_p|)}} = \sqrt{m|\mathcal{C}_p|} S_p(\mathbf{y}), \quad (34)$$

which measures the watermark strength after cumulatively incorporating all tokens mapped to the first  $p$  bit positions. In particular,  $z_b$  corresponds to the final  $z$ -score computed over the entire text.

By the central limit theorem,  $z_p$  converges in distribution to  $\mathcal{N}(0, 1)$  under the null hypothesis  $H_0$  for each  $p$ . For watermarked text, tokens aligned with the embedded message bits contribute biased scores within each bit position, causing the cumulative statistic to deviate from zero as additional positions are incorporated. In multi-bit watermarking with symmetric signed scores  $d_{t, \ell} \in \{-1, +1\}$ , the overall mean bias may cancel out when the numbers of embedded 0- and 1-bits are balanced, making the final signed statistic  $z_b$  close to zero. However, the watermark does not induce a uniform mean shift; instead, it creates structured, position-dependent biases. Consequently, detection remains effective when using two-sided or position-aware statistics, such as  $|z_p|$ ,  $\max_p |z_p|$ , or the energy  $\sum_{p=1}^b z_p^2$ , which are robust to sign cancellation.

In practice, we find that replacing  $d_{t, \ell}$  with a max-based heuristic,  $d_{t, \ell} \triangleq \max(g_\ell(y_t, r), \bar{g}_\ell(y_t, r))$ , often yields stronger empirical detection performance. While this hard selection improves the effective signal-to-noise ratio by suppressing noisy contributions, it introduces a positive bias under  $H_0$  and therefore does not yield a properly calibrated  $z$ -score.

## H. More Experimental Results

To evaluate message-level decoding accuracy, we use the Message Extracted Rate (ME Rate). We further apply a Hamming error-correcting code (Hamming, 1950) to alleviate the sensitivity of ME Rate to a small number of bit errors. As reported in

## WorldCup Sampling for Multi-bit LLM Watermarking

Table 4. Comparison of different multi-bit watermark performance, where  $\ominus$  denotes the baselines,  $\bullet$  denotes our watermark method.

Bit Length	Watermark	LLAMA3-8B-BASE												GEMMA2-9B-BASE												
		MAX 128 TOKENS						MAX 256 TOKENS						MAX 128 TOKENS						MAX 256 TOKENS						
		AUC $\uparrow$	ME Rate $\uparrow$	PPL $\downarrow$	Time (s) $\downarrow$	AUC $\uparrow$	ME Rate $\uparrow$	PPL $\downarrow$	Time (s) $\downarrow$	AUC $\uparrow$	ME Rate $\uparrow$	PPL $\downarrow$	Time (s) $\downarrow$	AUC $\uparrow$	ME Rate $\uparrow$	PPL $\downarrow$	Time (s) $\downarrow$	AUC $\uparrow$	ME Rate $\uparrow$	PPL $\downarrow$	Time (s) $\downarrow$	AUC $\uparrow$	ME Rate $\uparrow$	PPL $\downarrow$	Time (s) $\downarrow$	
16 bits	$\ominus$ MPAC	0.999	0.520	16.25	0.049	0.996	0.785	13.56	0.087	0.980	0.305	13.69	0.045	0.985	0.500	12.00	0.070									
	$\ominus$ SegMark	0.993	0.815	15.88	0.551	0.995	0.995	12.94	0.839	0.979	0.510	13.19	1.234	0.999	0.905	10.94	2.402									
	$\ominus$ BiMark	1.000	0.750	14.34	0.026	1.000	0.860	11.25	0.044	1.000	0.410	11.06	0.031	0.999	0.620	9.625	0.039									
	$\bullet$ Ours ( $k = 1$ )	1.000	0.915	7.938	0.007	1.000	0.970	6.563	0.012	0.998	0.710	7.250	0.007	0.994	0.860	6.344	0.012									
	$\bullet$ Ours ( $k = 2$ )	0.998	0.940	12.94	0.008	1.000	0.990	10.94	0.013	1.000	0.850	10.94	0.009	1.000	0.965	9.563	0.012									
24 bits	$\ominus$ MPAC	0.996	0.175	16.75	0.052	0.997	0.445	14.00	0.074	0.972	0.085	13.69	0.044	0.959	0.190	12.00	0.070									
	$\ominus$ SegMark	0.947	0.450	17.13	0.721	0.992	0.975	13.38	0.804	0.849	0.190	13.19	1.670	0.974	0.695	10.13	2.853									
	$\ominus$ BiMark	1.000	0.280	14.34	0.027	1.000	0.700	11.34	0.036	0.998	0.085	11.63	0.030	0.990	0.415	9.938	0.043									
	$\bullet$ Ours ( $k = 1$ )	0.999	0.505	7.938	0.008	0.996	0.820	6.625	0.016	0.998	0.280	7.375	0.008	0.993	0.610	5.844	0.013									
	$\bullet$ Ours ( $k = 2$ )	1.000	0.710	12.84	0.008	1.000	0.885	10.75	0.013	0.999	0.500	10.44	0.008	1.000	0.815	9.125	0.016									
32 bits	$\ominus$ MPAC	0.997	0.035	16.75	0.051	0.996	0.255	14.00	0.090	0.947	0.005	13.81	0.046	0.940	0.025	11.63	0.074									
	$\ominus$ SegMark	0.909	0.240	16.63	0.642	0.989	0.840	12.94	1.053	0.824	0.025	12.75	1.751	0.955	0.465	10.25	3.362									
	$\ominus$ BiMark	1.000	0.055	13.91	0.026	1.000	0.425	12.38	0.040	0.996	0.005	12.00	0.031	0.989	0.115	9.938	0.041									
	$\bullet$ Ours ( $k = 1$ )	0.996	0.100	8.250	0.008	1.000	0.565	6.547	0.014	0.996	0.060	7.125	0.008	0.998	0.355	6.250	0.015									
	$\bullet$ Ours ( $k = 2$ )	0.998	0.390	13.28	0.011	1.000	0.800	10.56	0.013	1.000	0.105	10.66	0.009	1.000	0.565	9.500	0.013									
48 bits	$\ominus$ MPAC	0.993	0.000	16.63	0.057	0.990	0.010	13.19	0.078	0.936	0.000	14.00	0.048	0.914	0.000	12.19	0.076									
	$\ominus$ SegMark	0.837	0.000	16.38	0.725	0.968	0.340	15.56	1.381	0.770	0.000	13.38	2.668	0.900	0.030	9.938	3.382									
	$\ominus$ BiMark	1.000	0.000	14.25	0.027	0.999	0.060	11.63	0.037	0.985	0.000	11.53	0.029	0.975	0.000	10.03	0.040									
	$\bullet$ Ours ( $k = 1$ )	0.998	0.000	7.750	0.009	1.000	0.140	6.688	0.014	0.983	0.000	7.000	0.009	0.985	0.010	5.938	0.013									
	$\bullet$ Ours ( $k = 2$ )	0.999	0.025	12.84	0.009	1.000	0.310	11.44	0.014	0.996	0.015	10.50	0.009	0.998	0.130	9.313	0.014									

Table 4, WorldCup consistently outperforms existing baselines across most settings. Fig.7 shows that our method achieves more reliable detection while preserving better text quality. Additional robustness results (Fig.8 and Fig. 9) indicate that sentence-level attacks (e.g., back-translation and paraphrasing) are more harmful to multi-bit watermarking than word-level attacks (e.g., word deletion and synonym substitution). This is inherent to bit-allocation-based schemes, as sentence-level transformations disrupt the contextual alignment required to recover token-level bit information. Improving robustness to such attacks remains an open challenge.

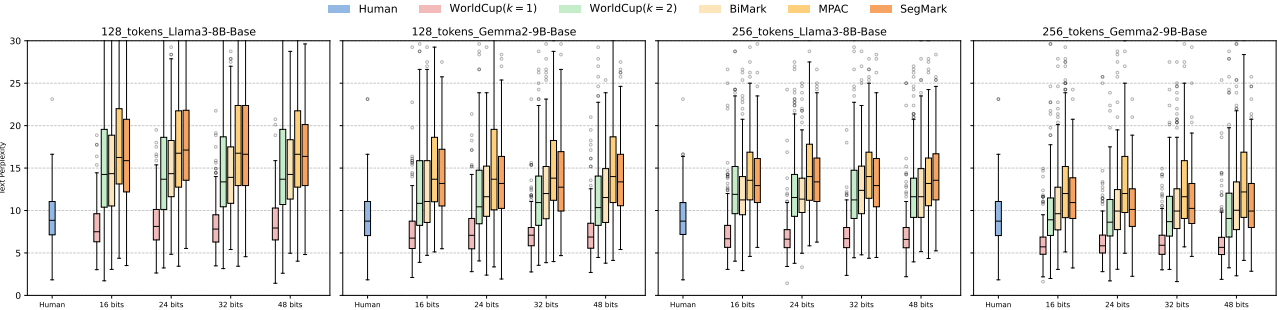


Figure 7. The comparison of PPL across different multi-bit watermarking methods on LLaMA3-8B and Gemma2-9B.

The numerical results corresponding to Fig. 5 and Fig. 6 are reported in Table 5 and Table 6, respectively. Based on these experimental results, we select the hyperparameter  $\alpha = 1.2$  and set the number of  $g$ -value functions to 2, as this configuration provides a favorable trade-off among bit accuracy, watermark detectability, and text quality.

Table 5. The numerical results of the ablation study on different components of WorldCup.

Model	C4 DATASET														
	16 bits			24 bits			32 bits			48 bits			64 bits		
+ Watermark	Best F1 $\uparrow$	Bit Acc $\uparrow$	PPL $\downarrow$	Best F1 $\uparrow$	Bit Acc $\uparrow$	PPL $\downarrow$	Best F1 $\uparrow$	Bit Acc $\uparrow$	PPL $\downarrow$	Best F1 $\uparrow$	Bit Acc $\uparrow$	PPL $\downarrow$	Best F1 $\uparrow$	Bit Acc $\uparrow$	PPL $\downarrow$
<b>LLAMA3-8B-BASE</b>															
+ WorldCup ( $k = 1$ , ours)	0.997	0.986	6.688	0.997	0.958	6.688	0.992	0.930	6.844	0.998	0.880	6.563	0.997	0.807	6.594
+ WorldCup ( $k = 1$ , w/o comp.)	0.995	0.949	6.813	1.000	0.907	6.656	1.000	0.874	7.031	1.000	0.797	6.563	0.998	0.754	6.750
+ WorldCup ( $k = 2$ , w/o entropy)	1.000	0.996	28.38	1.000	0.989	28.75	1.000	0.983	28.75	1.000	0.963	27.00	0.998	0.929	28.75
+ WorldCup ( $k = 2$ , w/o minus)	0.940	0.933	5.906	0.946	0.895	6.094	0.910	0.853	6.063	0.884	0.802	6.063	0.870	0.765	5.875
+ WorldCup ( $k = 2$ , w/o comp.)	0.995	0.986	14.13	0.995	0.975	13.56	0.995	0.937	13.56	0.992	0.904	14.13	0.987	0.868	13.19
+ WorldCup ( $k = 2$ , ours, $\lambda$ )	0.995	0.988	9.813	0.980	0.974	10.13	0.985	0.956	9.313	0.953	0.923	9.813	0.954	0.873	9.406
+ WorldCup ( $k = 2$ , ours, 1.2 $\lambda$ )	0.990	0.990	11.25	0.985	0.977	11.25	0.988	0.965	10.94	0.970	0.930	11.06	0.963	0.888	11.44
+ WorldCup ( $k = 2$ , ours, 1.5 $\lambda$ )	0.998	0.995	14.81	0.992	0.981	14.81	0.993	0.973	15.38	0.985	0.936	15.38	0.975	0.909	14.44
+ WorldCup ( $k = 2$ , ours, 2.0 $\lambda$ )	1.000	0.998	49.00	1.000	0.995	49.75	1.000	0.989	48.63	1.000	0.963	49.38	1.000	0.938	49.38

## WorldCup Sampling for Multi-bit LLM Watermarking

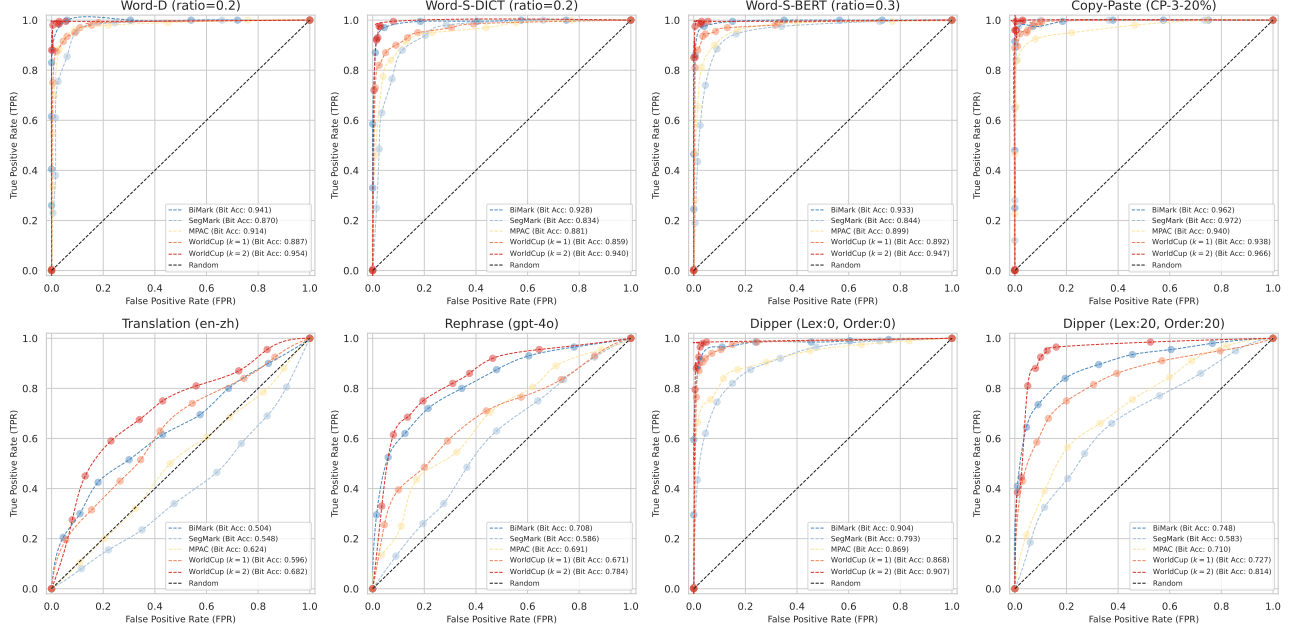


Figure 8. The AUROC curves under different attacks on LLaMA3-8B-Base model (16 bits).

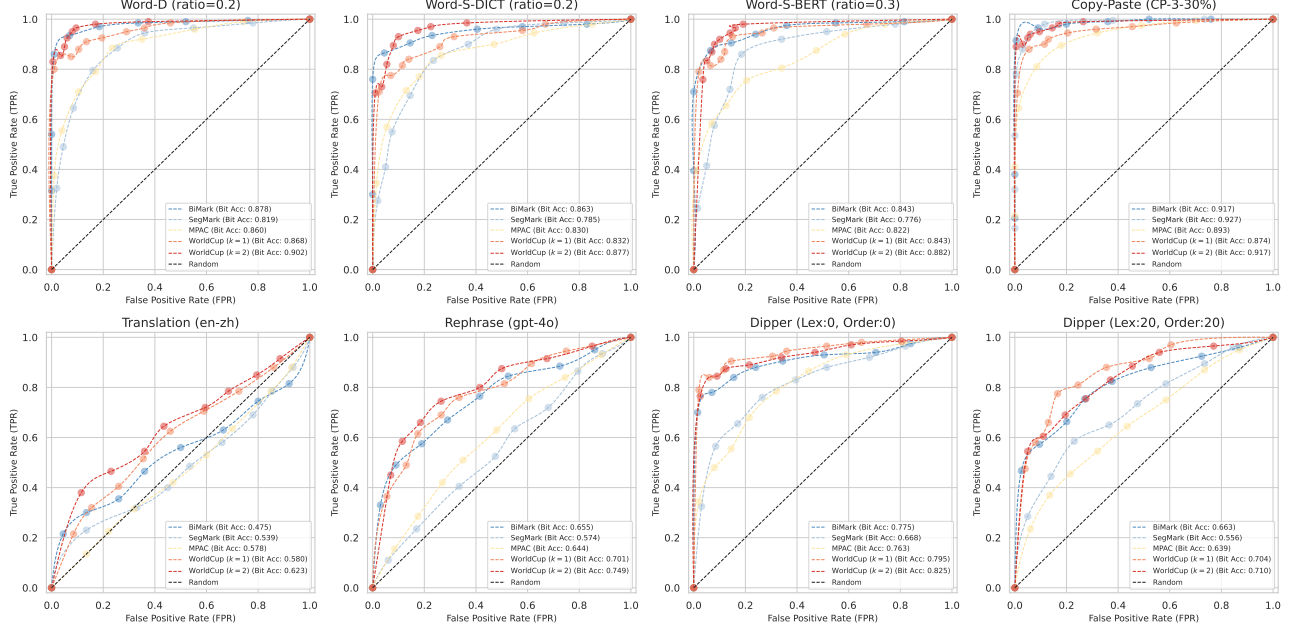


Figure 9. The AUROC curves under different attacks on Gemma2-9B-Base model (16 bits).

Table 6. The effect of  $g$ -value function number on different LLMs.

Model	$g\_function\_num=1$		$g\_function\_num=2$		$g\_function\_num=3$		$g\_function\_num=4$		$g\_function\_num=6$		$g\_function\_num=8$	
	Bit Acc $\uparrow$	Enc Time $\downarrow$										
<b>LLAMA3-8B-BASE</b>	-	-	-	-	-	-	-	-	-	-	-	-
WorldCup (24 bit)	0.980	0.083	0.995	0.213	0.993	0.287	0.990	0.371	0.986	0.533	0.985	0.690
WorldCup (48 bit)	0.917	0.069	0.975	0.203	0.966	0.285	0.958	0.366	0.950	0.530	0.939	0.689
<b>GEMMA2-9B-BASE</b>	-	-	-	-	-	-	-	-	-	-	-	-
WorldCup (24 bit)	0.943	0.079	0.991	0.214	0.988	0.296	0.986	0.374	0.975	0.532	0.971	0.691
WorldCup (48 bit)	0.871	0.080	0.951	0.215	0.945	0.294	0.933	0.377	0.926	0.531	0.910	0.693

## I. Additional Analysis

### I.1. Entropy Analysis

From the results in Table 1, we observe that existing multi-bit watermarking methods achieve substantially lower bit decoding accuracy on Gemma2-9B-Base than on LLaMA3-8B-Base. To better understand this phenomenon, we conduct an entropy-based analysis. Specifically, we visualize the average token-level entropy for each sample during text generation, as illustrated in Fig. 10. The results clearly indicate that Gemma2-9B-Base produces tokens with consistently lower entropy, aligning with prior findings that low-entropy text is inherently more challenging for watermark embedding. A plausible explanation is that Gemma2-9B-Base, owing to its larger parameter scale compared to LLaMA3-8B-Base, generates tokens with higher confidence, thereby reducing entropy and limiting the effective embedding capacity for multi-bit watermarks.

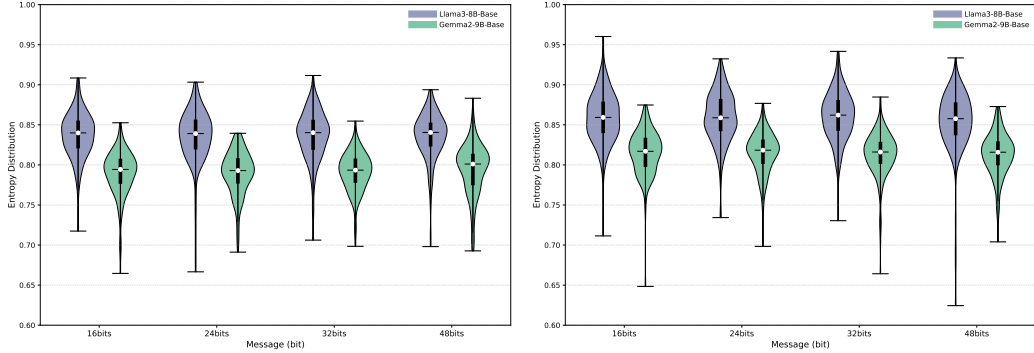


Figure 10. The comparison of spike entropy between LLaMA3-8B-Base and Gemma2-9B-Base across different message bits

### I.2. Distortionary and Non-distortionary $g$ -value Functions

According to SynthID (Dathathri et al., 2024), we define distortionary and non-distortionary  $g$ -value functions as follows:

**Definition I.1.** A sampling algorithm  $\mathcal{S} : \Delta \mathcal{V} \times \mathcal{R} \rightarrow \mathcal{V}$  is (single-token) non-distortionary if for any probability distribution  $p \in \Delta \mathcal{V}$  and token  $x \in \mathcal{V}$ :

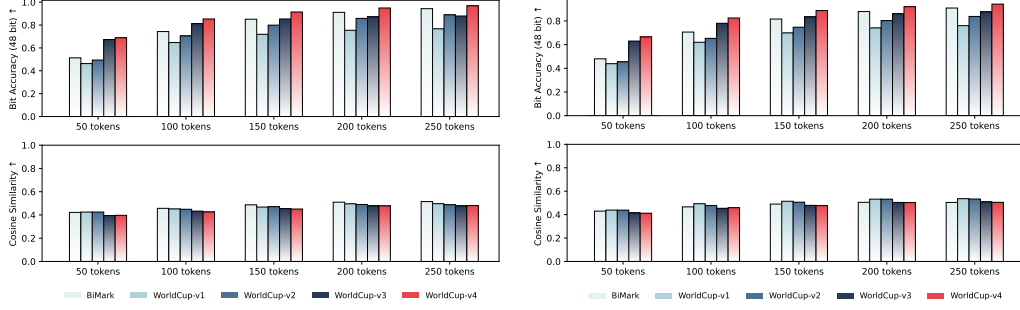
$$\mathbb{E}_{r \sim \text{Unif}(\mathcal{R})} [\mathbb{P}(\mathcal{S}(p, r) = x)] = p(x) \quad (35)$$

If  $\mathcal{S}$  is not non-distortionary, we call it distortionary.

Therefore, following the design of non-distortionary and distortionary  $g$ -value functions in SynthID, we evaluate their performance in the multi-bit watermarking setting. The results are summarized in Fig. 11 and Table 7. Specifically, WorldCup-v1, v2, v3, and v4 in the figure correspond to the configurations ( $k = 1$ , non-distortionary), ( $k = 1$ , distortionary), ( $k = 2$ , non-distortionary), and ( $k = 2$ , distortionary) in the Table 7, respectively. We observe that the non-distortionary setting yields higher cosine similarity between the generated watermarked text and the ground truth compared to the distortionary setting, at the cost of reduced bit accuracy. Consequently, in practical scenarios, the choice between these two settings can be made based on application-specific requirements. Unless otherwise stated, our experiments primarily adopt the distortionary configuration.

Table 7. The comparison of distortionary  $g$ -value function and non-distortionary  $g$ -value function.

Model	50 tokens			100 tokens			C4 DATASET			200 tokens			250 tokens		
	Best F1 $\uparrow$	Bit Acc $\uparrow$	Cos Sim $\uparrow$	Best F1 $\uparrow$	Bit Acc $\uparrow$	Cos Sim $\uparrow$	Best F1 $\uparrow$	Bit Acc $\uparrow$	Cos Sim $\uparrow$	Best F1 $\uparrow$	Bit Acc $\uparrow$	Cos Sim $\uparrow$	Best F1 $\uparrow$	Bit Acc $\uparrow$	Cos Sim $\uparrow$
<b>LLAMA3-8B-BASE</b>															
+ BiMark	0.972	0.513	0.422	0.998	0.743	0.457	1.000	0.851	0.487	1.000	0.911	0.510	1.000	0.943	0.515
+ WorldCup ( $k = 1$ , non-distortionary)	0.883	0.463	0.425	0.916	0.647	0.452	0.883	0.719	0.468	0.881	0.754	0.496	0.869	0.767	0.497
+ WorldCup ( $k = 1$ , distortionary)	0.935	0.494	0.425	0.967	0.705	0.449	0.980	0.799	0.471	0.992	0.858	0.490	0.990	0.889	0.488
+ WorldCup ( $k = 2$ , non-distortionary)	0.934	0.673	0.395	0.941	0.812	0.433	0.929	0.853	0.454	0.915	0.871	0.479	0.912	0.879	0.478
+ WorldCup ( $k = 2$ , distortionary)	0.947	0.689	0.397	0.995	0.853	0.426	0.997	0.914	0.451	1.000	0.949	0.478	1.000	0.968	0.481
<b>GEMMA2-9B-BASE</b>															
+ BiMark	0.949	0.480	0.430	0.988	0.706	0.466	0.995	0.816	0.490	1.000	0.879	0.505	0.998	0.909	0.504
+ WorldCup ( $k = 1$ , non-distortionary)	0.807	0.439	0.439	0.864	0.620	0.493	0.888	0.699	0.514	0.909	0.741	0.532	0.879	0.760	0.536
+ WorldCup ( $k = 1$ , distortionary)	0.865	0.455	0.438	0.935	0.653	0.478	0.948	0.747	0.506	0.972	0.803	0.532	0.975	0.838	0.533
+ WorldCup ( $k = 2$ , non-distortionary)	0.870	0.630	0.415	0.950	0.780	0.454	0.958	0.834	0.479	0.962	0.861	0.504	0.959	0.876	0.508
+ WorldCup ( $k = 2$ , distortionary)	0.915	0.665	0.412	0.992	0.825	0.459	0.990	0.888	0.477	0.993	0.920	0.503	0.997	0.942	0.505


 Figure 11. The comparison of distortionary and non-distortionary  $g$ -value functions

### I.3. Different Detectors

Following SynthID Text (Dathathri et al., 2024), we consider two watermark detectors: mean detector (D1) and weighted-mean detector (D2).

The mean detector computes the average  $g$ -value across all tokens and all layers as

$$\text{MeanScore}(x) := \frac{1}{mT} \sum_{t=1}^T \sum_{\ell=1}^m g_{t,\ell}, \quad (36)$$

where  $T$  denotes the number of tokens and  $m$  the number of layers.

The weighted-mean detector assigns non-increasing weights  $\alpha_1 \geq \dots \geq \alpha_m \geq 0$  to different layers, with  $\sum_{\ell=1}^m \alpha_{\ell} = m$ :

$$\text{WeightedMeanScore}(x, \alpha) := \frac{1}{mT} \sum_{t=1}^T \sum_{\ell=1}^m \alpha_{\ell} g_{t,\ell}. \quad (37)$$

Specifically, we set  $\alpha_1 = \tau$ ,  $\alpha_2 = \tau - \frac{\tau-\mu}{m-1}$ ,  $\alpha_3 = \tau - 2\frac{\tau-\mu}{m-1}$ ,  $\dots$ ,  $\alpha_m = \mu$ , with  $\tau = 10$  and  $\mu = 1$ , and then renormalize the weights such that  $\sum_{\ell=1}^m \alpha_{\ell} = m$ .

We evaluate both detectors under  $k = 1$  and  $k = 2$  on the C4 and OpenGen datasets across varying token lengths. Figure 12 shows the corresponding detection curves, and the quantitative results are summarized in Table 8. Our results indicate that for  $k = 1$ , the weighted-mean detector consistently outperforms the mean detector, in agreement with the findings of SynthID. This is because the contribution of watermarking evidence from each layer diminishes as depth increases, making layer-wise weighting beneficial. However, for  $k = 2$ , this trend reverses, and the mean detector achieves superior performance. A plausible explanation is that the use of multiple  $g$ -functions alleviates the attenuation of watermark signals across layers, thereby diminishing the advantage of layer weighting.

Table 8. The comparison of mean watermark detector and weighted mean watermark detector on WorldCup.

Dataset	LLAMA3-8B-BASE									
	50 tokens		100 tokens		150 tokens		200 tokens		250 tokens	
+ Watermark	Best F1 $\uparrow$	Bit Acc $\uparrow$								
<b>C4 DATASET</b>	-	-	-	-	-	-	-	-	-	-
+ BiMark	$1.000 \pm 0.000$	$0.530 \pm 0.001$	$1.000 \pm 0.000$	$0.758 \pm 0.007$	$1.000 \pm 0.000$	$0.866 \pm 0.007$	$1.000 \pm 0.000$	$0.919 \pm 0.006$	$1.000 \pm 0.000$	$0.949 \pm 0.008$
+ WorldCup ( $k = 1$ , D1)	$0.931 \pm 0.039$	$0.509 \pm 0.009$	$0.980 \pm 0.010$	$0.736 \pm 0.010$	$0.985 \pm 0.015$	$0.832 \pm 0.002$	$0.995 \pm 0.005$	$0.879 \pm 0.002$	$0.995 \pm 0.005$	$0.906 \pm 0.001$
+ WorldCup ( $k = 1$ , D2)	$0.953 \pm 0.005$	$0.520 \pm 0.007$	$0.985 \pm 0.005$	$0.744 \pm 0.005$	$0.995 \pm 0.005$	$0.846 \pm 0.001$	$0.990 \pm 0.010$	$0.895 \pm 0.004$	$0.995 \pm 0.005$	$0.918 \pm 0.000$
+ WorldCup ( $k = 2$ , D1)	$0.985 \pm 0.015$	$0.697 \pm 0.004$	$0.995 \pm 0.005$	$0.869 \pm 0.001$	$1.000 \pm 0.000$	$0.930 \pm 0.002$	$1.000 \pm 0.000$	$0.957 \pm 0.003$	$1.000 \pm 0.000$	$0.974 \pm 0.001$
+ WorldCup ( $k = 2$ , D2)	$0.975 \pm 0.015$	$0.683 \pm 0.003$	$1.000 \pm 0.000$	$0.857 \pm 0.006$	$1.000 \pm 0.000$	$0.914 \pm 0.001$	$1.000 \pm 0.000$	$0.948 \pm 0.003$	$1.000 \pm 0.000$	$0.966 \pm 0.002$
<b>OPENGEN DATASET</b>	-	-	-	-	-	-	-	-	-	-
+ BiMark	$0.995 \pm 0.005$	$0.538 \pm 0.008$	$1.000 \pm 0.000$	$0.765 \pm 0.004$	$1.000 \pm 0.000$	$0.774 \pm 0.006$	$1.000 \pm 0.000$	$0.927 \pm 0.006$	$1.000 \pm 0.000$	$0.955 \pm 0.003$
+ WorldCup ( $k = 1$ , D1)	$0.934 \pm 0.006$	$0.517 \pm 0.004$	$0.975 \pm 0.015$	$0.749 \pm 0.006$	$1.000 \pm 0.000$	$0.848 \pm 0.006$	$1.000 \pm 0.000$	$0.896 \pm 0.004$	$1.000 \pm 0.000$	$0.927 \pm 0.004$
+ WorldCup ( $k = 1$ , D2)	$0.960 \pm 0.020$	$0.526 \pm 0.011$	$0.995 \pm 0.005$	$0.768 \pm 0.006$	$1.000 \pm 0.000$	$0.868 \pm 0.001$	$1.000 \pm 0.000$	$0.915 \pm 0.002$	$1.000 \pm 0.000$	$0.943 \pm 0.000$
+ WorldCup ( $k = 2$ , D1)	$0.975 \pm 0.005$	$0.702 \pm 0.005$	$1.000 \pm 0.000$	$0.871 \pm 0.005$	$1.000 \pm 0.000$	$0.930 \pm 0.004$	$1.000 \pm 0.000$	$0.959 \pm 0.001$	$1.000 \pm 0.000$	$0.972 \pm 0.006$
+ WorldCup ( $k = 2$ , D2)	$0.985 \pm 0.005$	$0.684 \pm 0.004$	$1.000 \pm 0.000$	$0.850 \pm 0.003$	$1.000 \pm 0.000$	$0.909 \pm 0.002$	$1.000 \pm 0.000$	$0.949 \pm 0.003$	$1.000 \pm 0.000$	$0.966 \pm 0.000$

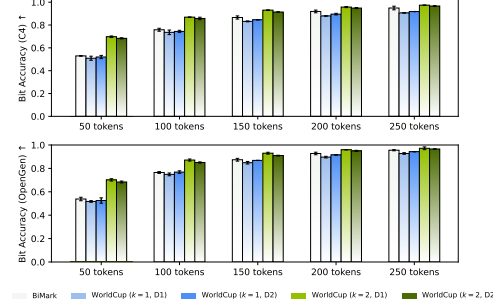


Figure 12. The comparison of mean detector and weighted mean detector.

#### I.4. WorldCup Sampling Layers

To investigate the impact of the number of layers in WorldCup, we conducted experiments with different layer counts  $m = 5, 10, 20, 30, 50$  on LLaMA3-8B-Base and Gemma2-9B-Base, with results summarized in Table 9. Empirically, a layer count of  $m = 30$  yields relatively optimal performance, consistent with findings from SynthID-Text (Dathathri et al., 2024). Lower layer counts generally lead to decreased decoding accuracy, while increasing the number of layers exhibits a diminishing returns effect. The number of layers, however, has no significant impact on perplexity (PPL). Therefore, in this work, we primarily adopt  $m = 30$  for our experiments.

 Table 9. The result of Worldcup sampling across different number of layers  $m$ .

Model	layers $m = 5$				layers $m = 10$				C4 DATASET				layers $m = 20$				layers $m = 30$				layers $m = 50$			
	Best F1 $\uparrow$	Bit Acc $\uparrow$	PPL $\downarrow$	Time (s) $\downarrow$	Best F1 $\uparrow$	Bit Acc $\uparrow$	PPL $\downarrow$	Time (s) $\downarrow$	Best F1 $\uparrow$	Bit Acc $\uparrow$	PPL $\downarrow$	Time (s) $\downarrow$	Best F1 $\uparrow$	Bit Acc $\uparrow$	PPL $\downarrow$	Time (s) $\downarrow$	Best F1 $\uparrow$	Bit Acc $\uparrow$	PPL $\downarrow$	Time (s) $\downarrow$	Best F1 $\uparrow$	Bit Acc $\uparrow$	PPL $\downarrow$	Time (s) $\downarrow$
+ Watermark																								
<b>LLAMA3-8B-BASE</b>																								
+ WorldCup ( $k = 1$ )	0.954	0.931	5.688	0.011	0.998	0.972	6.188	0.011	0.995	0.985	6.625	0.011	1.000	0.987	6.563	0.011	0.998	0.984	7.063	0.011				
+ WorldCup ( $k = 2$ )	0.995	0.990	9.250	0.011	1.000	0.994	9.250	0.012	0.997	0.991	10.13	0.012	1.000	0.995	10.94	0.012	0.997	0.985	16.00	0.012				
<b>GEMMA2-9B-BASE</b>																								
+ WorldCup ( $k = 1$ )	0.932	0.883	5.719	0.011	0.975	0.933	5.938	0.011	0.993	0.957	6.078	0.012	0.997	0.972	6.125	0.013	0.980	0.963	6.031	0.012				
+ WorldCup ( $k = 2$ )	0.997	0.978	8.250	0.011	0.993	0.978	8.500	0.011	0.993	0.983	8.375	0.012	0.997	0.984	9.500	0.012	1.000	0.977	10.94	0.012				

In addition, we examine the effect of the number of leaves  $N$ , as reported in Table 10. The results indicate that setting  $N = 2$  provides the best trade-off between message decoding accuracy and text quality.

 Table 10. The result of Worldcup sampling across different number of leaves  $N$ .

Model	leaves $N = 1$				leaves $N = 2$				C4 DATASET				leaves $N = 3$				leaves $N = 4$					
	Best F1 $\uparrow$	Bit Acc $\uparrow$	PPL $\downarrow$	Time (s) $\downarrow$	Best F1 $\uparrow$	Bit Acc $\uparrow$	PPL $\downarrow$	Time (s) $\downarrow$	Best F1 $\uparrow$	Bit Acc $\uparrow$	PPL $\downarrow$	Time (s) $\downarrow$	Best F1 $\uparrow$	Bit Acc $\uparrow$	PPL $\downarrow$	Time (s) $\downarrow$	Best F1 $\uparrow$	Bit Acc $\uparrow$	PPL $\downarrow$	Time (s) $\downarrow$		
+ Watermark																						
<b>LLAMA3-8B-BASE</b>																						
+ WorldCup (16 bit)	0.670	0.495	5.500	0.011	0.998	0.985	6.719	0.011	1.000	0.998	15.38	0.011	1.000	1.000	53.75	0.012						
+ WorldCup (24 bit)	0.672	0.492	5.500	0.012	0.997	0.958	6.781	0.012	1.000	0.988	15.88	0.012	1.000	0.994	60.00	0.012						
+ WorldCup (32 bit)	0.670	0.493	5.500	0.012	0.995	0.925	6.875	0.013	1.000	0.972	15.63	0.013	1.000	0.991	61.75	0.013						
+ WorldCup (48 bit)	0.668	0.469	5.469	0.014	0.990	0.875	6.547	0.013	1.000	0.933	16.25	0.014	1.000	0.968	58.00	0.014						

#### I.5. Different Activation Function

We evaluate three activation functions in Eq.6, namely ReLU, Sigmoid, and Tanh. The results are reported in Table 11. Overall, the choice of activation function leads to comparable performance trends, and all variants exhibit a consistent trade-off between bit-level detection accuracy and text quality measured by perplexity. Specifically, ReLU exhibits relatively stronger detection performance due to its linear behavior for positive inputs; however, this gain is accompanied by a noticeable degradation in text quality. In contrast, Tanh and Sigmoid introduce nonlinear saturation, resulting in more conservative modulation and better preservation of generation quality. Since entropy values are non-negative, Tanh effectively normalizes them into the interval  $[0, 1]$ , whereas Sigmoid maps them into a narrower range of  $[0.5, 1]$ , which limits the dynamic range of modulation. Based on these considerations, we adopt the Tanh activation function in our method. Combined with a fixed scaling factor  $\alpha = 1.2$ , this choice provides a balanced trade-off between detection accuracy and text quality, while allowing stable and interpretable control of watermark strength in practice.

Table 11. The comparison of different activation functions on C4 dataset.

Model	C4 DATASET														
	16 bits			24 bits			32 bits			48 bits			64 bits		
+ Watermark	Best F1 $\uparrow$	Bit Acc $\uparrow$	PPL $\downarrow$	Best F1 $\uparrow$	Bit Acc $\uparrow$	PPL $\downarrow$	Best F1 $\uparrow$	Bit Acc $\uparrow$	PPL $\downarrow$	Best F1 $\uparrow$	Bit Acc $\uparrow$	PPL $\downarrow$	Best F1 $\uparrow$	Bit Acc $\uparrow$	PPL $\downarrow$
<b>LLAMA3-8B-BASE</b>															
+ WorldCup (ReLU, $\alpha = 0.8$ )	1.000	0.989	10.75	1.000	0.974	10.94	1.000	0.959	10.56	0.997	0.921	10.50	0.995	0.885	11.06
+ WorldCup (ReLU, $\alpha = 1$ )	1.000	0.991	11.44	1.000	0.987	11.72	1.000	0.971	12.00	1.000	0.936	12.19	0.997	0.899	12.38
+ WorldCup (Sigmoid, $\alpha = 1$ )	0.997	0.988	9.719	1.000	0.970	9.813	1.000	0.956	9.500	0.990	0.913	9.719	0.997	0.870	9.500
+ WorldCup (Sigmoid, $\alpha = 1.2$ )	1.000	0.990	11.06	0.997	0.979	11.25	1.000	0.963	11.44	1.000	0.925	11.63	1.000	0.891	11.44
+ WorldCup (Tanh, $\alpha = 1$ )	1.000	0.984	9.500	0.995	0.966	9.813	0.995	0.951	9.625	0.992	0.914	9.875	0.997	0.871	9.625
+ WorldCup (Tanh, $\alpha = 1.2$ )	0.997	0.991	10.84	0.995	0.976	10.75	0.995	0.956	10.25	0.997	0.918	10.94	0.995	0.889	10.66
<b>GEMMA2-9B-BASE</b>															
+ WorldCup (ReLU, $\alpha = 0.8$ )	0.997	0.960	8.375	0.993	0.930	8.500	0.990	0.911	8.188	0.985	0.871	8.375	0.983	0.822	8.000
+ WorldCup (ReLU, $\alpha = 1$ )	0.987	0.967	9.250	0.992	0.955	9.063	0.990	0.924	9.125	0.992	0.886	9.406	0.982	0.841	9.188
+ WorldCup (Sigmoid, $\alpha = 1$ )	0.990	0.968	8.375	0.992	0.940	7.750	0.992	0.914	7.938	0.977	0.867	8.375	0.980	0.827	8.250
+ WorldCup (Sigmoid, $\alpha = 1.2$ )	1.000	0.968	9.406	0.993	0.957	9.313	0.992	0.924	9.313	0.990	0.879	9.813	0.987	0.835	9.625
+ WorldCup (Tanh, $\alpha = 1$ )	0.995	0.962	7.750	0.995	0.934	7.688	0.992	0.901	7.875	0.977	0.853	7.750	0.972	0.813	7.875
+ WorldCup (Tanh, $\alpha = 1.2$ )	0.993	0.970	8.844	0.990	0.941	8.500	0.982	0.916	8.688	0.992	0.869	8.500	0.988	0.826	8.500

## I.6. Key Generation Hyperparameters

During watermark generation, both the `no_repeat_ngram_size` and the window size significantly affect multi-bit watermark performance, since the random seed for embedding is derived from hashing tokens within a context window. If text diversity is too low (e.g., `no_repeat_ngram_size = 0`), identical seeds are repeatedly used, leading to uneven bit allocation across tokens and poor decoding accuracy (Table 12). However, increasing diversity does not always help: setting `no_repeat_ngram_size = 1` severely degrades fluency, as reflected by high perplexity. Balancing decoding accuracy and text quality, we set `no_repeat_ngram_size = 4`. Moreover, window size also influences robustness by determining the extent of context used in hashing. Empirically, larger windows reduce robustness under attacks (Table 13 and Table 14). We therefore use a window size of 2 to achieve a favorable trade-off between robustness and fluency.

 Table 12. The effect of different `no_repeat_ngram_size` on multi-bit watermarking methods.

Watermark	LLAMA3-8B-BASE														
	no_repeat_ngram_size=0	no_repeat_ngram_size=1	no_repeat_ngram_size=2	no_repeat_ngram_size=3	no_repeat_ngram_size=4	no_repeat_ngram_size=0	no_repeat_ngram_size=1	no_repeat_ngram_size=2	no_repeat_ngram_size=3	no_repeat_ngram_size=4	no_repeat_ngram_size=0	no_repeat_ngram_size=1	no_repeat_ngram_size=2	no_repeat_ngram_size=3	no_repeat_ngram_size=4
DBiMark	5.356	0.947	6.375	20.00	1.000	45.25	18.03	0.993	15.63	8.890	0.994	12.56	7.804	0.992	11.81
WorldCup ( $k = 1$ )	5.036	0.885	3.070	20.00	1.000	34.25	17.88	0.987	9.500	7.715	0.981	7.344	7.202	0.978	6.625
WorldCup ( $k = 2$ )	6.110	0.947	7.750	20.00	1.000	62.75	18.92	0.996	18.88	8.794	0.996	15.38	7.929	0.994	14.25

 Table 13. The effect of different window size  $c$  across our framework WorldCup on LLaMA3-8B-Base.

Watermark	LLAMA3-8B-BASE															
	window_size $c = 1$		window_size $c = 2$		window_size $c = 3$		window_size $c = 4$		window_size $c = 1$		window_size $c = 2$		window_size $c = 3$		window_size $c = 4$	
+ Attack	TPR $\uparrow$	FPR $\downarrow$	F1 $\uparrow$	Bit Acc $\uparrow$	TPR $\uparrow$	FPR $\downarrow$	F1 $\uparrow$	Bit Acc $\uparrow$	TPR $\uparrow$	FPR $\downarrow$	F1 $\uparrow$	Bit Acc $\uparrow$	TPR $\uparrow$	FPR $\downarrow$	F1 $\uparrow$	Bit Acc $\uparrow$
WORLD CUP ( $k = 1$ )	0.995	0.005	0.995	0.951	1.000	0.000	1.000	0.983	0.995	0.000	0.997	0.984	0.990	0.000	0.995	0.987
+ Word-D (ratio=0.2)	0.985	0.020	0.983	0.907	0.960	0.000	0.980	0.933	0.930	0.005	0.961	0.911	0.895	0.020	0.935	0.873
+ Word-S-DICT (ratio=0.2)	0.965	0.025	0.970	0.895	0.930	0.005	0.961	0.908	0.960	0.065	0.948	0.868	0.845	0.070	0.883	0.842
+ Word-S-BERT (ratio=0.3)	0.970	0.025	0.972	0.893	0.950	0.000	0.974	0.924	0.930	0.030	0.949	0.906	0.900	0.020	0.938	0.871
+ Copy-Paste (CP-3-30%)	0.880	0.025	0.924	0.886	0.910	0.000	0.953	0.926	0.925	0.015	0.954	0.931	0.885	0.015	0.932	0.913
+ Translation (en-zh)	0.990	0.975	0.668	0.605	0.990	0.960	0.671	0.603	0.985	0.955	0.670	0.563	0.980	0.965	0.666	0.538
+ Rephrase (GPT-4o)	0.870	0.250	0.821	0.742	0.735	0.325	0.714	0.729	0.885	0.630	0.704	0.657	0.805	0.565	0.679	0.634
+ Dipper-1 (lex=0, order=0)	0.945	0.020	0.962	0.881	0.940	0.035	0.952	0.904	0.910	0.045	0.931	0.887	0.885	0.020	0.929	0.873
+ Dipper-2 (lex=20, Dipper=20)	0.895	0.110	0.893	0.793	0.865	0.180	0.846	0.772	0.765	0.130	0.807	0.738	0.770	0.295	0.746	0.698
WORLD CUP ( $k = 2$ )	0.995	0.020	0.988	0.974	1.000	0.000	1.000	0.991	1.000	0.000	1.000	0.993	1.000	0.000	1.000	0.994
+ Word-D (ratio=0.2)	0.995	0.055	0.971	0.941	0.975	0.000	0.987	0.949	0.975	0.010	0.982	0.933	0.980	0.035	0.973	0.905
+ Word-S-DICT (ratio=0.2)	0.980	0.050	0.966	0.920	0.975	0.020	0.977	0.942	0.940	0.050	0.945	0.909	0.925	0.035	0.944	0.888
+ Word-S-BERT (ratio=0.3)	0.995	0.055	0.971	0.923	0.980	0.035	0.973	0.940	0.945	0.045	0.950	0.922	0.975	0.060	0.958	0.897
+ Copy-Paste (CP-3-30%)	0.920	0.055	0.932	0.909	0.925	0.045	0.939	0.940	0.950	0.010	0.969	0.955	0.900	0.010	0.942	0.936
+ Translation (en-zh)	0.850	0.625	0.687	0.676	0.990	0.960	0.671	0.636	0.960	0.905	0.670	0.589	0.995	0.975	0.670	0.582
+ Rephrase (GPT-4o)	0.725	0.080	0.803	0.783	0.850	0.330	0.780	0.735	0.830	0.425	0.736	0.693	0.810	0.570	0.681	0.666
+ Dipper-1 (lex=0, order=0)	0.970	0.060	0.956	0.890	0.970	0.035	0.968	0.911	0.945	0.055	0.945	0.903	0.860	0.035	0.908	0.883
+ Dipper-2 (lex=20, Dipper=20)	0.860	0.080	0.887	0.798	0.825	0.165	0.829	0.790	0.845	0.390	0.756	0.719	0.765	0.330	0.730	0.693

## I.7. Counting-based Decoding vs. Confidence-aware Decoding

To rigorously demonstrate that the proposed confidence-aware decoding outperforms conventional counting-based decoding, we compare the decoding accuracy of WorldCup under both strategies, as reported in Table 15. The results clearly show that confidence-aware decoding consistently achieves higher accuracy across different embedded message bit lengths. This improvement fundamentally stems from its ability to mitigate the adverse influence of low-entropy tokens and instead rely

Table 14. The effect of different window size  $c$  across our framework WorldCup on Gemma2-9B-Base.

Watermark	GEMMA2-9B-BASE															
	window_size $c = 1$				window_size $c = 2$				window_size $c = 3$				window_size $c = 4$			
	TPR $\uparrow$	FPR $\downarrow$	F1 $\uparrow$	Bit Acc $\uparrow$	TPR $\uparrow$	FPR $\downarrow$	F1 $\uparrow$	Bit Acc $\uparrow$	TPR $\uparrow$	FPR $\downarrow$	F1 $\uparrow$	Bit Acc $\uparrow$	TPR $\uparrow$	FPR $\downarrow$	F1 $\uparrow$	Bit Acc $\uparrow$
<b>WORLD CUP (<math>k = 1</math>)</b>	0.995	0.015	0.990	0.909	0.995	0.010	0.993	0.943	0.995	0.000	0.997	0.973	1.000	0.005	0.998	0.974
+ Word-D (ratio=0.2)	0.955	0.030	0.962	0.872	0.875	0.085	0.893	0.868	0.860	0.050	0.901	0.848	0.830	0.105	0.858	0.813
+ Word-S-DICT (ratio=0.2)	0.945	0.075	0.936	0.853	0.890	0.165	0.866	0.832	0.945	0.235	0.867	0.827	0.810	0.170	0.818	0.784
+ Word-S-BERT (ratio=0.3)	0.930	0.025	0.951	0.851	0.925	0.140	0.896	0.843	0.830	0.055	0.881	0.847	0.815	0.150	0.830	0.828
+ Copy-Paste (CP-3-30%)	0.875	0.030	0.919	0.836	0.880	0.030	0.921	0.874	0.885	0.025	0.927	0.879	0.885	0.040	0.919	0.884
+ Translation (en-zh)	0.990	0.970	0.669	0.590	1.000	0.990	0.669	0.580	0.995	0.990	0.667	0.552	0.995	1.000	0.664	0.516
+ Rephrase (GPT-4o)	0.790	0.280	0.763	0.712	0.760	0.335	0.726	0.701	0.800	0.460	0.708	0.681	0.920	0.750	0.689	0.647
+ Dipper-1 (lex=0, order=0)	0.925	0.070	0.927	0.781	0.825	0.030	0.889	0.795	0.819	0.055	0.874	0.817	0.760	0.070	0.831	0.798
+ Dipper-2 (lex=20, Dipper=20)	0.840	0.140	0.848	0.716	0.790	0.175	0.804	0.704	0.845	0.480	0.727	0.688	0.880	0.640	0.698	0.655
<b>WORLD CUP (<math>k = 2</math>)</b>	0.970	0.020	0.975	0.947	0.995	0.000	0.997	0.968	0.995	0.000	0.997	0.983	0.995	0.000	0.997	0.984
+ Word-D (ratio=0.2)	0.950	0.085	0.934	0.909	0.935	0.045	0.944	0.905	0.915	0.060	0.927	0.887	0.905	0.065	0.919	0.858
+ Word-S-DICT (ratio=0.2)	0.905	0.060	0.921	0.877	0.845	0.045	0.894	0.882	0.860	0.060	0.896	0.869	0.855	0.110	0.870	0.824
+ Word-S-BERT (ratio=0.3)	0.910	0.060	0.924	0.896	0.850	0.045	0.897	0.878	0.865	0.060	0.899	0.867	0.815	0.110	0.847	0.830
+ Copy-Paste (CP-3-30%)	0.910	0.050	0.929	0.886	0.895	0.010	0.939	0.900	0.895	0.015	0.937	0.909	0.910	0.010	0.948	0.905
+ Translation (en-zh)	0.995	1.000	0.664	0.641	0.995	0.995	0.666	0.602	0.990	0.970	0.669	0.588	0.975	0.945	0.668	0.537
+ Rephrase (GPT-4o)	0.795	0.255	0.776	0.756	0.825	0.575	0.688	0.709	0.935	0.795	0.685	0.690	0.965	0.875	0.680	0.634
+ Dipper-1 (lex=0, order=0)	0.905	0.165	0.874	0.805	0.825	0.045	0.882	0.825	0.795	0.065	0.855	0.803	0.785	0.095	0.835	0.775
+ Dipper-2 (lex=20, Dipper=20)	0.890	0.290	0.817	0.715	0.865	0.400	0.764	0.710	0.840	0.545	0.704	0.649	0.875	0.645	0.694	0.626

more heavily on high-entropy tokens, which provide more reliable statistical evidence for decoding. This observation is also consistent with conclusions drawn in prior zero-bit watermarking studies, such as EWD (Lu et al., 2024), further validating the effectiveness of entropy-aware decoding strategies.

Table 15. The comparison of counting-based decoding and confidence-aware decoding.

Model	C4 DATASET																			
	16 bits				24 bits				32 bits				48 bits				64 bits			
	Best F1 $\uparrow$	Bit Acc $\uparrow$	PPL $\downarrow$	Best F1 $\uparrow$	Bit Acc $\uparrow$	PPL $\downarrow$	Best F1 $\uparrow$	Bit Acc $\uparrow$	PPL $\downarrow$	Best F1 $\uparrow$	Bit Acc $\uparrow$	PPL $\downarrow$	Best F1 $\uparrow$	Bit Acc $\uparrow$	PPL $\downarrow$	Best F1 $\uparrow$	Bit Acc $\uparrow$	PPL $\downarrow$		
<b>LLAMA3-8B-BASE</b>																				
+ WorldCup ( $k = 1$ , counting-based)	0.982	0.971	6.688	0.985	0.933	6.625	0.966	0.897	6.969	0.965	0.844	6.750	0.925	0.771	6.594					
+ WorldCup ( $k = 1$ , confidence-aware)	0.998	0.984	6.625	0.997	0.961	6.750	0.995	0.930	7.000	0.992	0.875	6.563	0.990	0.813	6.547					
+ WorldCup ( $k = 2$ , counting-based)	0.931	0.978	11.00	0.926	0.959	11.16	0.908	0.925	11.06	0.883	0.886	11.44	0.889	0.843	11.44					
+ WorldCup ( $k = 2$ , confidence-aware)	1.000	0.990	11.00	1.000	0.982	11.25	1.000	0.962	11.16	1.000	0.925	11.44	1.000	0.887	11.16					

## I.8. Algorithm

### Algorithm 2 WorldCup Message Decoding (Confidence-Aware)

- 1: **Input:** watermarking key  $\xi$  and hash seed  $r_t$ , total message length  $b$ ,  $2^k$ -ray,  $g$ -value function families  $\{\mathbf{g}_j, \bar{\mathbf{g}}_j\}_{j=1}^k$
- 2: Compute number of message symbols  $B \leftarrow b/k$
- 3: Initialize decoded message symbols  $\hat{\mathbf{m}} \in \{0, \dots, 2^k - 1\}^B$
- 4: Use  $(r_t, \xi)$  to map each token  $y_t$  to a message position  $p_t \in \{0, \dots, B - 1\}$
- 5: Group tokens by message position:  $\mathcal{S}_p = \{y_t \mid p_t = p\}$
- 6: **for**  $p = 0$  to  $B - 1$  **do**
- 7:     **for**  $j = 1$  to  $k$  **do**
- 8:         Compute confidence scores by averaging over the group:  $s_j^p \leftarrow \frac{1}{|\mathcal{S}_p|} \sum_{y_t \in \mathcal{S}_p} g_j(y_t)$ ,  $\bar{s}_j^p \leftarrow \frac{1}{|\mathcal{S}_p|} \sum_{y_t \in \mathcal{S}_p} \bar{g}_j(y_t)$
- 9:     **end for**
- 10:    Decode the  $2^k$ -ray message symbol:  $\hat{m}_p \leftarrow \sum_{j=1}^k 2^{k-j} \mathbb{I}(s_j^p < \bar{s}_j^p)$
- 11: **end for**
- 12: Assemble decoded symbols into message sequence:  $\hat{\mathbf{m}} \leftarrow (\hat{m}_0, \hat{m}_1, \dots, \hat{m}_{B-1})$
- 13: **Return** decoded message symbols  $\hat{\mathbf{m}}$

## J. Case Study

### J.1. Llama3-8B-Base Examples

#### Prompt (C4 Dataset)

Applications for entrance in the Fall of 2019 are now open. We will begin to evaluate applications on January 15, 2019. If your application is not

#### Natural Text (C4 Dataset)

received by then, it may not be evaluated. Please note that we do not typically admit for Spring or Summer admission. Offers are usually made between February and April 15. All applicants are considered for department support via research assistantships, teachings assistantships, and merit-based scholarships. Virtually all graduate students are supported for the academic year and in many cases during the summer term as well. Once the Graduate Admissions Committee has made a final decision on your application they will notify you via the email address that is on your application. There is no minimum GRE or GPA requirement. However, to be competitive for assistantships and scholarships, students need a GPA of at least 3.0, a combined verbal and quantitative score on the GRE of at least 300, and an analytical writing score on the GRE of at least 3.5. The average GRE score for students that were accepted into our program for Fall 2018 was 316.

#### Unwatermarked Text (Llama3-8B-Base)

complete by that date we will not be able to guarantee you an interview. Click here to begin an application. Please visit the requirements tab above for details about how to complete an application. The deadline for submitting applications for Fall, 2019 is March 31, 2019. A maximum of two interviews a week will be held every Tuesday at 1:00 p.m. and 3:00 p.m., and Wednesday at 9:00 a.m. and 1:00p.m. You may not request interview dates. There is no interview in the Spring. Interviewers are assigned by the Office of Admission. You will not be interviewed by anyone that you request for an interview.

#### Watermarked Text (Message: 1101000010110000 Bit Accuracy: 1.0 k=2)

complete or received before January 15, you will be placed in the second round of applications. Please be aware there is limited or no amount of spots for second round applications. Please be aware that all our students for the U.S. and Canada are in class by April 1, for non-residents this is 2 weeks later. We do not keep our spots open for the full year. If you cannot get into Canada by April 1 you cannot join our Program. We will not make arrangements for you to join the Program at a later date. For spots that become available, even if we have already started the Program, only students who have the ability to be in Canada by April 13 will be admitted.

#### Prompt (C4 Dataset)

Independent Bank Corp. (nasdaq global select market:INDB), parent of Rockland Trust Company, today announced 2018 fourth quarter net income of

#### Natural Text (C4 Dataset)

\$29.9 million, or \$1.07 per diluted share, compared to net income of \$33.0 million, or \$1.20 per diluted share, reported in the prior quarter of 2018. Excluding merger and acquisition expenses incurred in the fourth and third quarters of 2018 related to the MNB Bancorp (MNB) merger which closed in November 2018 and the Blue Hills Bancorp (BHB) merger announced on September 20, 2018, operating net income was \$35.9 million, or \$1.29 per diluted share during the fourth quarter of 2018 compared to \$34.9 million, or \$1.27 per diluted share during the third quarter of 2018. Full year net income was \$121.6 million, or \$4.40 on a diluted earnings per share basis, an increase of \$34.4 million, or 39.5%, as compared to the prior year. In addition, full year operating net income was \$129.8.

**Unwatermarked Text (Llama3-8B-Base)**

\$35.8 million, or \$0.78 per diluted share, an increase of 2.7% and 3.3% from the \$34.9 million, or \$1.02 per diluted share, reported for the 2017 fourth quarter. For the 2018 full year, net income increased 20.1% to \$137.4 million, or \$3.03 per diluted share, compared to \$114.3 million, or \$2.88 per diluted share, for the 2018 year ended December 31, 2017. The 2018 fourth quarters and full year included \$5.6 million in total credit loss expense, compared to the corresponding prior year amounts of \$4.0 million and \$16.6 million. The 2017 fourth quarters and full years included \$3.6 million and \$6.3 million, respectively, in additional expense for the tax effect of deferred tax liabilities associated with the impact of the change in U.S. federal corporate tax rates from 35% to 21% as a result of the Tax Cuts and Jobs Act. “During the quarter we completed a successful acquisition of the 17 branches and other deposits from Eastern Bank.

**Watermarked Text (Message: 00111111010010000101010 Bit Accuracy: 0.75 k=2)**

\$26.6 million, or \$0.79 per share, compared to \$23.5 million, or \$1.40 per share, in the prior year’s fourth quarter. For the full year 2018, net income was \$101.7 million, or \$3.06 per share, compared with \$85.2 million, or \$5.29 per share, in 2017. The Company’s 2018 performance was impacted by the non-cash charge of \$10.7 million, which was added back to net income in the calculation of earnings per share, to establish a valuation allowance against its deferred tax assets. This charge was partially offset by a \$6.1 million, or \$10.1 million on an after-tax basis, increase in net interest income due to lower interest expense. Pre-tax, pre-provision net revenue increased 15.1%, driven by growth in loans and deposits, higher non-interest income and lower non-interest expense.

**J.2. Gemma2-9B-Base Examples****Prompt (C4 Dataset)**

Our no. 1 sneaker of 2014 just got a serious upgrade in the form of the adidas Pure Boost ZG Prime. We first

**Natural Text (C4 Dataset)**

previewed this sneaker in January, and now the next-gen of Pure Boost has arrived. This model mixes a full-length Boost midsole with a layer of EVA on the outsole to produce what adidas calls a floating sensation, hence the Zero Gravity’s; (ZG) part of its name. That’s not the only key feature here, as this version of the Pure Boost ZG also features a Primeknit upper for a cozy and adaptive sock-like fit. It’s then finished off with leather tabs at the tongue and heel, adding a premium touch to an otherwise sporty silhouette. If for some reason this Primeknit variation isn’t quite your cup of tea—or out of your budget—there’s also a less expensive mesh-based version dropping this summer. The adidas Pure Boost ZG Prime is now available in black.

**Unwatermarked Text (Gemma2-9B-Base)**

laid eyes on the Adidas PureBoost ZG Prime at the recent 2015 PGA Show where the model made its debut on the feet of former World No. 1 and 3-time Major champion, Ernie Els. For the 2016 season, Ernie Els has teamed up with Adidas Golf and will don the PureBoost ZG on his feet during the Major season. It’s no secret that adidas Pure Boost technology is the best when it comes to running. The adidas PureBoost ZG and PureBoost ZG Primes boast a flexible woven upper that provides a sock-like fit with minimal movement. adidas Pureboost ZG Prime are made with Primeknit upper, featuring woven technology for flexible fit. adidas Pure Boost ZG. Adidas Pure Boost ZG/Primes are engineered with Primeknit upper, featuring flexible material and delivering comfortable fit. adidas has now released the PureBoost Z and ZG Primes. Adidas PureBoost ZG will also launch this winter in six color options. adidas just released the PureBoost Prime, and now the ZG model is set to make its debut in the near future.

**Watermarked Text (Message: 1101101011101010 Bit Accuracy: 1.0 k=2)**

saw the Pure Boost ZG back in July, and one of our editors was lucky enough to try them out during the 2015 World Championships in Beijing, China. The adidas Pure Boost Zg Prime is an update to the most popular running shoe of 2004, the Pure Boost Zg. The Zg Prime has a more streamlined upper and a wider base for a more comfortable fit. The new upper is made of 2 layers of a breathable material, with a 3rd layer of support at the medial side of the shoe. The adidas pure boost zg prime is the latest in a long line of running shoes from adidas. It features a Boost midsole and a Primeknit upper. The shoe also features an EVA midsole for cushioning and a Torsion System for stability. The adidas Zg Prime is a running shoe that features an Air Max unit, a Boost midsole, and a Primeknit upper. The shoe is available in two colorways: Black/White/Grey and White/Black/Grey. The black version features a suede upper with a leather overlay, while the white version features a mesh upper with a leather liner. Both shoes feature a Boost midsole with an Air Max unit.

**Prompt (C4 Dataset)**

A child in Florida has become the first person to die of the flu this season, according to state health officials. State epidemiologists say the

**Natural Text (C4 Dataset)**

child had not been vaccinated and was otherwise healthy before getting sick with the flu. The child, who tested positive for influenza B, died sometime during the week of Sept. 30, although privacy concerns prevent officials from saying exactly where, CBS affiliate WTSP-TV reports. Last flu season, 183 children in the U.S. died from flu or flu-related causes. That's the most since the Centers for Disease Control and Prevention (CDC) began keeping these records in 2004. Overall, an estimated 80,000 Americans died from flu last season. CBS News medical contributor Dr. Tara Narula says this latest news should be a wake-up call to parents to get their children vaccinated. "What this is a strong clear message to parents about the importance of vaccination," she told "CBS This Morning." "This vaccine is safe. It is the most effective tool we have. And we know of the pediatric deaths last year, 80 percent were in kids who were unvaccinated.

**Unwatermarked Text (Gemma2-9B-Base)**

child died from influenza B. That's different from the type of flu A that caused death and illness in children last year. The CDC says 17 children died of the flu in the 2009-10 flu season, 11 of them from the H1N1 strain, or swine flu. Last year 18 children in 10 states died of swine flu, according to the AAP. That's in addition to eight children who died from the flu last year.

**Watermarked Text (Message: 011001110110011011100110 Bit Accuracy: 0.958 k=2)**

child died of flu complications, but did not specify the age of the child or where in the state they lived. It's unclear if the child had been vaccinated against the flu. A spokesperson for the Florida Department of Health said the state does not release information about the individual flu cases. The U.S. Centers for Disease Control and Prevention currently reports that the flu has spread to 46 states, and has killed at least 11 people so far this season. According to the CDC, the flu has hit people hardest 50 to 64 years old. The CDC also reports that in the last week, 45 people out of every 100,000 have sought medical treatment for flu-like symptoms. That's up from 26 the week before. Health officials say this year's flu strain is particularly. The CDC says 75 percent of people who die from the flu each year are 65 or older. Some experts say this year'll be flu season. But they say there's still time to get vaccinated against the flu, and they urge people to do so.